Article

Not peer-reviewed version

Transcriptional Analysis of a Tripartite Interaction Between a Plant, a Pathogenic Fungus and Its Bacterial Control Agent

Paúl Alán Báez-Astorga , Abraham Cruz-Mendívil , Juan Luis Figueroa-Castro , Itzel Guadalupe López-Soto , Jesús Eduardo Cazares-Álvarez , Josefat Gregorio-Jorge , Carlos Ligne Calderón-Vázquez , Ignacio Eduardo Maldonado-Mendoza *

Posted Date: 31 October 2025

doi: 10.20944/preprints202510.2343.v1

Keywords: RNA-seq; maize transcriptome; endophyte; *Bacillus cereus*; *Fusarium verticillioides*; differentially expressed genes; biological control; plant-microbe interactions

Article

Transcriptional Analysis of a Tripartite Interaction Between a Plant, a Pathogenic Fungus and Its Bacterial Control Agent

Paúl Alán Báez-Astorga [1,†], Abraham Cruz-Mendívil [1,†], Juan Luis Figueroa-Castro [2], Itzel Guadalupe López-Soto [3], Jesús Eduardo Cazares-Álvarez [1], Josefat Gregorio-Jorge [4], Carlos Ligne Calderón-Vázquez [3] and Ignacio Eduardo Maldonado-Mendoza [3,*]

[1] SECIHTI - Instituto Politécnico Nacional, CIIDIR Unidad Sinaloa, Guasave, México
[2] Universidad Autónoma de Occidente (UAdeO), Unidad Regional Guasave, Guasave, México
[3] Departamento de Biotecnología Agrícola, Centro Interdisciplinario de Investigación para el Desarrollo Integral Regional (CIIDIR) Unidad Sinaloa, Instituto Politécnico Nacional, Guasave, México
[4] SECIHTI - Comisión Nacional del Agua, Ciudad de México, México
* Correspondence: ignacioemaldonado@yahoo.com.mx; Tel.: (+52) 6878729626
† These authors contributed equally to this work and share first authorship.

Abstract

One open question regarding plant-microbe interactions is how a plant interacts molecularly with both a beneficial microbe and a pathogenic fungus. This study used RNA-seq to investigate molecular responses in maize roots during a tripartite interaction with the fungal pathogen *Fusarium verticillioides* (*Fv*), which causes stalk, ear, and root rot, and the endophytic biocontrol agent *Bacillus cereus sensu lato* B25, known to suppress *Fv* and promote plant growth. Roots of seven-day-old maize inoculated with *Fv* (*Zm-Fv*), B25 (*Zm-B*25), and co-inoculated (*Zm-Fv-B*25) were compared to uninoculated control (*Zm*). Differential Gene Expression (DEG), Gene Ontology (GO) and KEGG analysis revealed distinct molecular responses. *Fv* suppressed plant pathways related to DNA and protein synthesis and impaired root development. In contrast, B25 triggered defense preparedness and growth-related responses. In the co-inoculation (*Zm-Fv-B*25), upregulated DEGs were associated with defense-related metabolic pathways, including jasmonic acid signaling and secondary metabolite biosynthesis, while also promoting plant growth. Co-expression networks using *Arabidopsis* orthologs supported these findings. This study is the first RNA-seq analysis of maize root molecular responses during the tripartite interaction with a fungal pathogen and its bacterial biocontrol agent, providing new directions for further research to understand the detailed molecular mechanisms underlying this interaction fully.

Keywords: RNA-seq; maize transcriptome; endophyte; *Bacillus cereus*; *Fusarium verticillioides*; differentially expressed genes; biological control; plant-microbe interactions

1. Introduction

Currently, over a billion tons of maize are produced every year, making it the most abundant cereal crop globally [1]. Maize is susceptible to different fungal pathogens, with *Fusarium verticillioides* (*Fv*) being the most common cause of stalk, ear and root rot (SERR) [2,3]. *Fv* is a versatile fungus that can infect maize either through seeds (vertical transmission), or by environmental causes such as dissemination through the soil, air or natural wounds inflicted by herbivores (horizontal transmission). As a hemibiotroph, *Fv* can either live harmlessly inside maize as a symptomless endophyte or cause disease as a necrotrophic pathogen [4,5]. *Fv* not only affects maize yield but also grain quality, due to contamination by mycotoxins [6].

 doi:10.20944/preprints202510.2343.v1

Due to increasing global concerns regarding the environment and the human health effects of synthetic agricultural chemicals (such as pesticides, fungicides, insecticides, and herbicides), there is a strong drive to identify sustainable ways to manage crop diseases [7]. Among such alternatives, the use of biological control agents (BCAs) is not only efficient in controlling target pests and diseases, but they also improve plant growth, development, and ultimately crop yields [8,9]. Bacterial endophytes from the genera *Bacillus*, *Paenibacillus*, *Burkholderia*, *Pseudomonas* and *Staphylococcus* have been successfully employed as BCAs to effectively control SERR caused by *Fv* on maize [10–13]. Endophytes are non-pathogenic microorganisms that inhabit the plant internal parts for at least part of their life cycle and are generally considered beneficial microorganisms due to their plant growth promotion and plant protection properties [14,15]. These beneficial microorganisms use several mechanisms to promote plant growth and act as biocontrol agents. To enhance plant growth, endophytes can fix nitrogen, solubilize phosphate and potassium, produce siderophores, and synthesize various phytohormones like auxins, cytokinins and gibberellins [14]. On the other hand, these endophytes can employ direct and indirect antagonism mechanisms for biocontrol. Indirect antagonism in biocontrol works by priming the host plant defenses, making them react faster and more powerfully when pathogens attack. In contrast, direct antagonism is achieved through mechanisms like hyperparasitism, predation, and the production of lytic enzymes and antibiotics [14,16].

The advantage that endophytes have over other biocontrol agents is their ability to colonize the internal tissues of plants, which allows them to share the same ecological niche as some phytopathogens inside the plant host, increasing their value as biocontrol candidates [14,15]. As an example of this, the maize endophytic biocontrol agent *Bacillus cereus* strain *B*25 colonizes the maize root vasculature [17], just like the phytopathogen *Fv* [4].

*B*25 has demonstrated effective control of *Fv* through *in vitro*, greenhouse, and field trials [9,13,18]. The genome of *B*25 possesses genes related to several antagonistic mechanisms against fungal pathogens, including the production of lytic enzymes (chitinases A and B, chitosanase and glycoside hydrolase), siderophores (petrobactin and bacillibactin), antibiotics (surfactin), and biofilm production [19]. These mechanisms have been biochemically and molecularly characterized and appear to be involved in the direct biocontrol of *B*25 over *Fv*, as all of them are induced during their direct interaction *in vitro* [13,20–22]. In addition, *B*25 contributes to the reduction of fumonisin levels and increases maize yield [9].

Although we understand the antagonism mechanisms used by *B*25 to control *Fv* (bacteria-fungus interaction) and the maize physiological responses when inoculated with *B*25 and challenged with *Fv*, the molecular mechanisms involved in the maize-*B*25-*Fv* tripartite interaction have not been investigated at the transcriptional level. To understand this tripartite interaction, and due to the complexity of capturing the molecular communication (mRNA) of microorganisms due to their proportion with respect to maize, this work focuses on the description of the molecular responses of maize regarding its interaction with the bacterial biocontrol agent and the fungal pathogen.

Here, we address the question of how a plant could simultaneously interact with a phytopathogenic fungus and a beneficial organism. Because studying interactions between three organisms is particularly challenging, we developed a model of the tripartite interaction between maize, the phytopathogenic fungus *Fv* (which causes SERR) and its biological control agent, the endophytic bacterium *B*25. RNA-seq is a method for understanding the molecular mechanisms underlying certain host-microorganism interactions [23]. By analyzing the maize transcriptome in response to inoculation with 1) the biocontrol endophyte *B*25 (*Zm-B*25), 2) the fungal pathogen *Fv* (*Zm-Fv*), and 3) both *B*25 and *Fv* (*Zm-B*25-*Fv*), we have identified key genes and molecular mechanisms involved in the maize-*B*25-*Fv* (*Zm-B*25-*Fv*) tripartite interaction.

 doi:10.20944/preprints202510.2343.v1

2. Results

2.1. B25 Mediated the Biocontrol of Fv and Enhanced Maize Plant Growth in the Tripartite Interaction

To confirm that the rolled paper seedling bioassay enabled initial host plant colonization, and to assess the physiological responses of the plant to each organism in bi- and tri-partite interactions, we microbiologically verified colonization and measured plantlet biomass and length. Microbial colonization was visually confirmed on disinfected maize roots (Supplementary Figure 1), with no growth on controls (*Zm*). Bipartite associations (*Zm-B25* and *Zm-Fv*) showed greater microbial growth than the tripartite interaction (*Zm-B25-Fv*). *Fv* inoculation (*Zm-Fv*) significantly reduced root length and fresh weight compared to other treatments (*Zm*, *Zm-B25*, *Zm-B25-Fv*) (Table 1). However, co-inoculation with *Fv* and *B25* (*Zm-B25-Fv*) promoted a significant increase in leaf length and fresh weight compared to all other conditions (*Zm*, *Zm-B25*, *Zm-Fv*).

Table 1. Growth parameters of maize plants from the tripartite assay seven days post infection (dpi).

Condition	Length (cm)		Fresh weight (g)	
	Leaf	Root	Leaf	Root
Zm	11.92^{b}	13.07^{a}	0.38^{b}	0.78^{a}
Zm-B25	11.27^{b}	12.52^{a}	0.34^{b}	0.78^{a}
Zm-Fv	11.52^{b}	**9.86^{b}**	0.34^{b}	**0.64^{b}**
Zm-B25-Fv	**14.28^{a}**	13.80^{a}	**0.47^{a}**	0.77^{a}

Zm: *Zea mays*; *B25*: *Bacillus cereus B25*; *Fv*: *Fusarium verticillioides* P03. Values indicate the average of five plants. Different letters indicate significant differences (Tukey's test $P \leq 0.05$). Bold values highlight statistically significant differences as described in the text.

2.2. RNA Sequencing of the Tripartite Assay

More than 162 million raw paired-end reads were obtained from the sequencing of the whole tripartite experiment, with an average of 20 million reads per sample (Table 2). After quality trimming (>Q20), an average of 98.49% of the reads was retained per library. Additionally, 95.93% of these filtered reads also achieved a quality score of >Q30. The mean values of unique and multiple mapped reads were 17,703,196 (87.28%) and 758,808 (3.71%), respectively.

Table 2. Summary of filtered and mapped reads obtained from the RNA-seq of maize root samples.

Sample	Raw Reads	Filtered Reads (Q>20)		Unique Mapped Reads	
Zm-2	13,742,216	13,534,709	(98.49%)	12,542,341	(91.27%)
Zm-3	21,273,970	20,839,981	(97.96%)	17,042,555	(80.11%)
Zm-B25-1	22,841,141	22,498,524	(98.50%)	19,719,075	(86.33%)
Zm-B25-2	27,395,643	27,003,885	(98.57%)	24,442,305	(89.22%)
Zm-Fv-1	19,155,891	18,880,046	(98.56%)	17,497,335	(91.34%)
Zm-Fv-3	18,080,786	17,815,902	(98.54%)	14,513,113	(80.27%)
Zm-B25-Fv-1	18,442,655	18.199,212	(98.68%)	16,495,370	(89.44%)
Zm-B25-Fv-3	21,465,145	21,166,779	(98.61%)	19,373,477	(90.26%)
Average	20,299,681	19,992,380	(98.49%)	17,703,196	(87.28%)

Zm: *Zea mays*; *B25*: *Bacillus cereus B25*; *Fv*: *Fusarium verticillioides* P03; Q: Phred quality score. Numbers after the condition name indicate the biological replicate. Filtered reads were mapped to the reference genome of maize B73 v5.

 doi:10.20944/preprints202510.2343.v1

A principal component analysis (PCA) was carried out to confirm consistency between biological replicates. One biological replicate from each of the four conditions (*Zm*, *Zm-B*25, Zm-*Fv* and *Zm-B*25-*Fv*) showed an atypical behavior and were thus removed, keeping two biological replicates from each condition as described in Materials and Methods section 2.5 (Supplementary Figure 2).

2.3. Global Transcriptome Profiles of Maize Roots from the Tripartite Assay

Expressed genes (EGs) were defined as those averaging at least 10 read counts across two biological replicates. Maize roots in the tripartite assay expressed 24,628 out of 44,303 predicted genes from the *Zea mays* B73 v5 genome, representing 55.59% of the genome (Table 3). Inoculation of maize roots with *B*25 and/or *Fv* induced the expression of a higher percentage of the genome compared to the control (*Zm*). Interestingly, maize root colonization by *B*25 (*Zm-B*25) caused the highest percentage of gene expression, with 57.36% (25,412 genes) of the genome. A comparative analysis across all conditions revealed a core of 22,576 (86.6%) common EGs. However, individual conditions showed distinct profiles: *Zm-B*25 exhibited the largest number of unique EGs (454, 1.7%), followed by *Zm* with 254 (1%), *Zm-Fv* with 215 (0.8%), and *Zm-B*25-*Fv* with 189 (0.7%) (Figure 1).

Table 3. Expressed genes (EGs) in maize roots of the tripartite assay.

Condition	Total EGs	Percentage of the genome[a]
Zm	23,625	53.33%
*Zm-B*25	25,412	57.36%
Zm-Fv	24,668	55.68%
*Zm-B*25-*Fv*	24,808	56.00%
Average	24,628	55.59%

Zm: *Zea mays*; *B*25: *Bacillus cereus B*25; *Fv*: *Fusarium verticillioides* P03. [a] Refers to the *Zea mays* B73 v5.0 genome (44,303 genes).

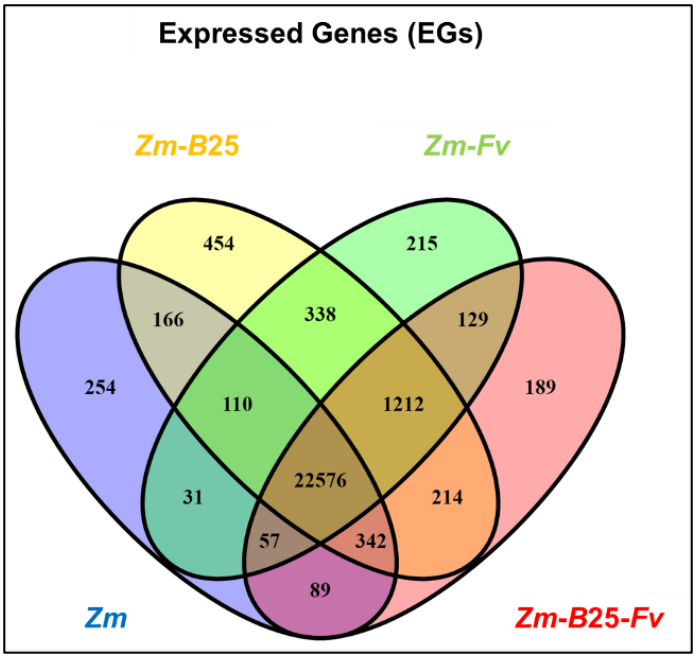

Figure 1. Venn diagram of common and uniquely expressed genes in the transcriptome of maize roots of the tripartite assay. *Zm*: *Zea mays*; *B*25: *Bacillus cereus B*25; *Fv*: *Fusarium verticillioides* P03. .

 doi:10.20944/preprints202510.2343.v1

Unique EGs from the interaction conditions were subjected to GO analysis. The results showed 11, 8 and 4 overrepresented terms for *Zm-B25*, *Zm-Fv*, and *Zm-B25-Fv*, respectively (Supplementary Table 3). Overrepresented terms within the unique EGs of *Zm-B25* were associated with the regulation of transcription and negative regulation of catalytic activity. Additionally, response to auxin also appeared as an overrepresented term in this interaction. On the other hand, overrepresented terms within the set of unique EGs in *Zm-Fv* were related to photosynthesis regulation, primary metabolic process, cell fate determination, and regulation of transcription. Finally, the terms overrepresented in *Zm-B25-Fv* unique EGs were associated with restructuring and growth of the actin cytoskeleton (Supplementary Table 3).

2.4. Differentially Expressed Genes Within and Among Maize Interactions

The number of DEGs for the *Zm-B25*, *Zm-Fv*, and *Zm-B25-Fv* conditions was 4,331, 5,473 and 2,334, respectively (Table 4, Supplementary Table 2). The three interactions shared a common core of 1,948 DEGs (Figure 2). The tripartite *Zm-B25-Fv* interaction showed the fewest unique DEGs (78), in contrast to the bipartite *Zm-B25* (653) and *Zm-Fv* (1,513) interactions, which exhibited more unique DEGs. Furthermore, *Zm-B25-Fv* shared 295 DEGs exclusively with the *Zm-Fv* interaction and only 13 with the *Zm-B25* interaction, while *Zm-B25* and *Zm-Fv* shared a substantial 1,717 DEGs.

Table 4. Differentially expressed genes (DEGs) in the interaction conditions (vs. control).

Condition	Total DEGs	Up-regulated	Down-regulated
Zm-B25	4331	3884 (89.68%)	447 (10.32%)
Zm-Fv	5473	4076 (74.47%)	1397 (25.53%)
Zm-B25-Fv	2334	2077 (88.98%)	257 (11.02%)

Zm: Zea mays; B25: Bacillus cereus B25; Fv: Fusarium verticillioides P03.

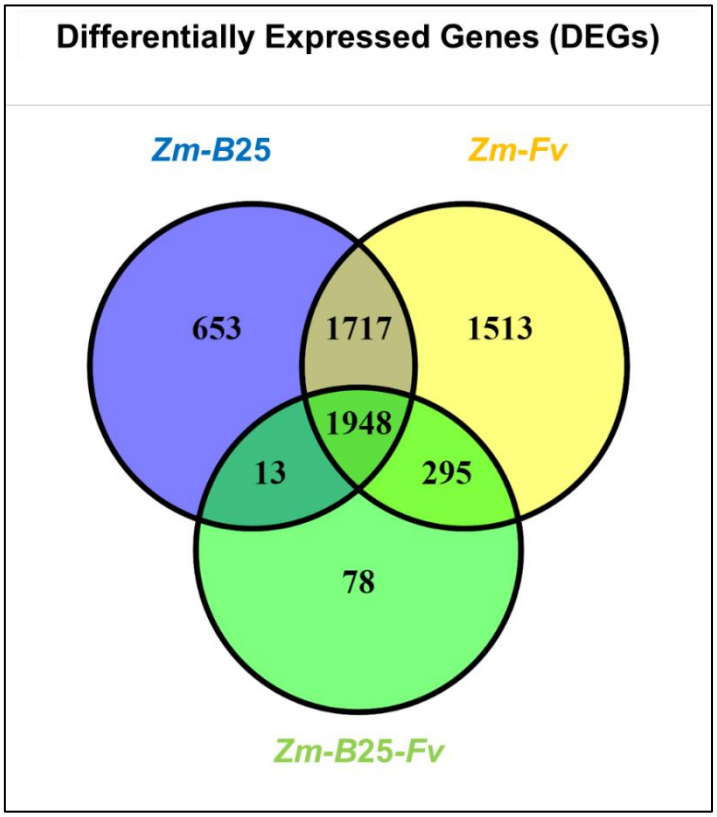

Figure 2. Differentially expressed genes (DEGs) in the tripartite interaction. Venn diagrams of common and unique DEGs between bi- and tri-partite interactions. *Zm*: *Zea mays*; *B25*: *Bacillus cereus B25*; *Fv*: *Fusarium verticillioides* P03.

 doi:10.20944/preprints202510.2343.v1

In general, the proportion of upregulated genes (>74%) was higher than the downregulated genes for all conditions (Table 4). Bacterial (*Zm-B*25) and bacterial-pathogen (*Zm-B*25-*Fv*) inoculation on maize resulted in gene expression patterns with approximately 89% of upregulated and only 10-11% of downregulated genes. In contrast, 25.64% of genes were repressed in *Zm-Fv* (Table 4).

By analyzing the number of up- and downregulated genes (both unique and shared) within each interaction, we gained a comprehensive understanding of the transcriptome's overall behavior in this study. Whereas 6 out of 7 Venn diagram sections displayed a common trend of more upregulated than downregulated genes (data not shown), only unique DEGs in *Zm-Fv* showed the opposite trend. In *Zm-Fv*, downregulated genes were more numerous (972; 64.24%) than upregulated genes (541; 35.75%). In summary, *Zm-Fv* had the highest number of DEGs, accumulating most of the unique DEGs as well as those shared with *Zm*-B25 and *Zm-B*25-*Fv*.

2.5. Overrepresentation Analysis: A General Approach

GO analysis revealed a significant overrepresentation (adjusted *p-value* <0.05) of 64 categories in the *Zm-B*25-*Fv* interaction, 90 categories in the *Zm-B*25 interaction, and 60 categories in the *Zm-Fv* interaction (Figure 3; Supplementary Table 4). The *Zm-Fv* interaction contained the highest number of DEGs (5,473), but it showed the lowest number of overrepresented categories. Overall, the overrepresented categories belonged mainly to Molecular Function (MF) with 54, followed by Biological Process (BP) with 38, and Cellular Compartment (CC) with 10. The three conditions shared 42 overrepresented categories. Notably, *Zm*-B*25* exhibited the highest number of unique overrepresented categories with 27, followed by *Zm-B*25-*Fv* with 8, and *Zm-Fv* with 5 (Figure 3).

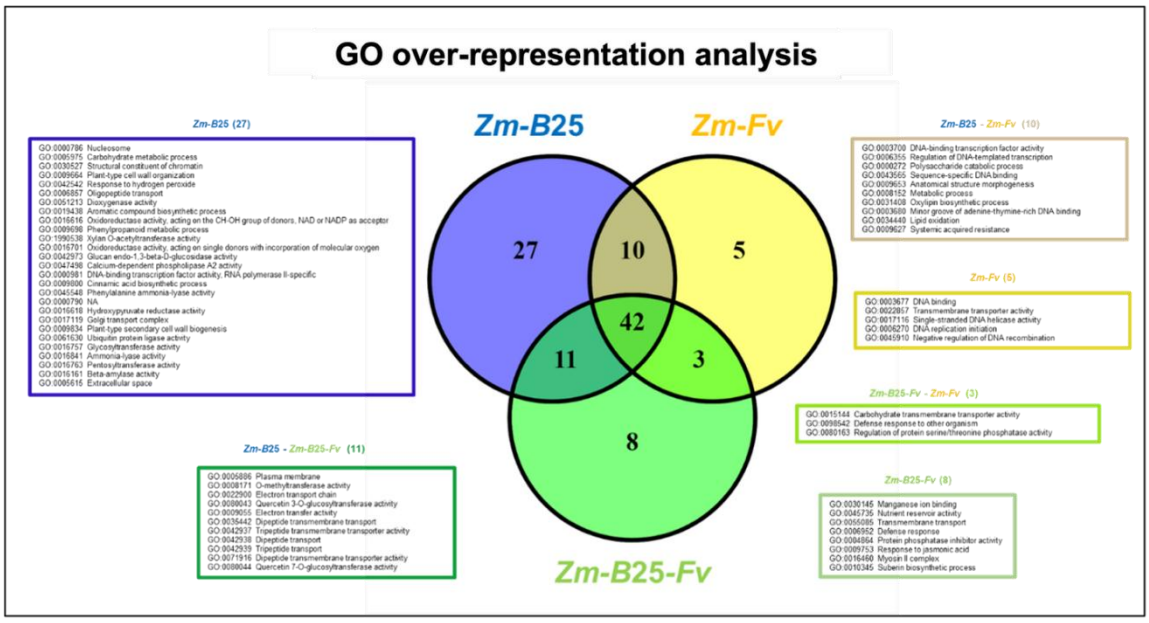

Figure 3. Venn diagram of unique and shared overrepresented Gene Ontology (GO) terms between the interactions. Boxes display the list of the overrepresented GO terms exclusive to one or shared by two interactions. The list of common GO terms (42) shared between the three interactions is shown in Supplementary Table 4.

Among the eight unique and overrepresented GO terms for *Zm-B*25-*Fv*, four corresponded to the BP category defense response (GO:0006952), and response to jasmonic acid (GO:0009753) appeared together with suberin biosynthetic process (GO:0010345) and transmembrane transport (GO:0055085) (Supplementary Table 4). The myosin II complex (GO:0016460) was the sole overrepresented term identified in the CC category, whereas nutrient reservoir activity (GO:0045735),

 doi:10.20944/preprints202510.2343.v1

protein phosphatase inhibitor activity (GO:0004864) and manganese ion binding (GO:0030145) were found in the MF category (Supplementary Table 4).

For the *Zm-B*25 interaction, the unique overrepresented GO terms in the BP category included those related to plant growth and development, such as aromatic compound biosynthetic process (GO:0019438), phenylpropanoid and carbohydrate metabolic process (GO:0009698 and GO:0005975) and plant-type secondary cell wall biogenesis (GO:0009834). In the MF category, a diverse set of overrepresented terms were identified, primarily related to transcription regulation (GO:0000981), catalysis of O-glycosil compounds (GO:001616 and GO:0042973), and transferase activity (ubiquitin (GO:0061630), as well as the pentosyl (GO:0016763), glycosil (GO:0016757) and acyl groups (GO:1990538), oxido-reductase activity (GO:0016616, GO:0016618, GO:0016701 and GO:0051213), calcium-dependent phospholipase A2 activity (GO:0047498), structural constituent of chromatin (GO:0030527), and ammonia-lyase activity (GO:0016841). The overrepresented terms for the CC category included extracellular space (GO:0005615), nucleosome (GO:0000786), chromatin (GO:0000785), and Golgi transport complex (GO:0017119).

In the *Zm-Fv* interaction, four out of the five unique overrepresented GO terms were associated with DNA replication (GO:0003677, GO:0017116, GO:0006270 and GO:0045910).

Interestingly, *Zm-B*25 and *Zm-Fv* shared 10 overrepresented GO terms (Figure 3, brown box). Several terms stood out within these overrepresented GO terms, such as those associated with transcription (GO:0003700, GO:0006355, GO:0043565), oxylipin biosynthesis (GO:0031408), and the systemic acquired resistance response (GO:0009627).

2.6. KEGG Analysis

KEGG analysis revealed 13, 19, and 20 overrepresented pathways in the *Zm-B*25-*Fv*, *Zm-B*25, and *Zm-Fv* interactions, respectively (Figure 4, Supplementary Table 5). Only *Zm-B25* (5) and *Zm-Fv* (6) exhibited uniquely overrepresented KEGG pathways. The five unique pathways identified in *Zm-B*25 were associated with plant growth and development (zma00905: brassinosteroid biosynthesis), signaling (zma00590: arachidonic acid metabolism, zma04016: MAPK signaling pathway - plant), amino acid metabolism (zma00250: alanine, aspartate and glutamate metabolism), and production of secondary metabolites (zma00944: flavone and flavonol biosynthesis). On the other hand, five out of the six unique overrepresented KEGG pathways in the *Zm-Fv* interaction were related to DNA replication and maintenance, including DNA replication (zma03030), homologous recombination (zma03440), base excision repair (zma03410), and non-homologous end-joining (zma03450). Additionally, ribosome biogenesis in eukaryotes (zma03008) was a unique overrepresented pathway. The remaining unique KEGG pathway was motor proteins (zma04814) (Figure 4, Supplementary Table 5).

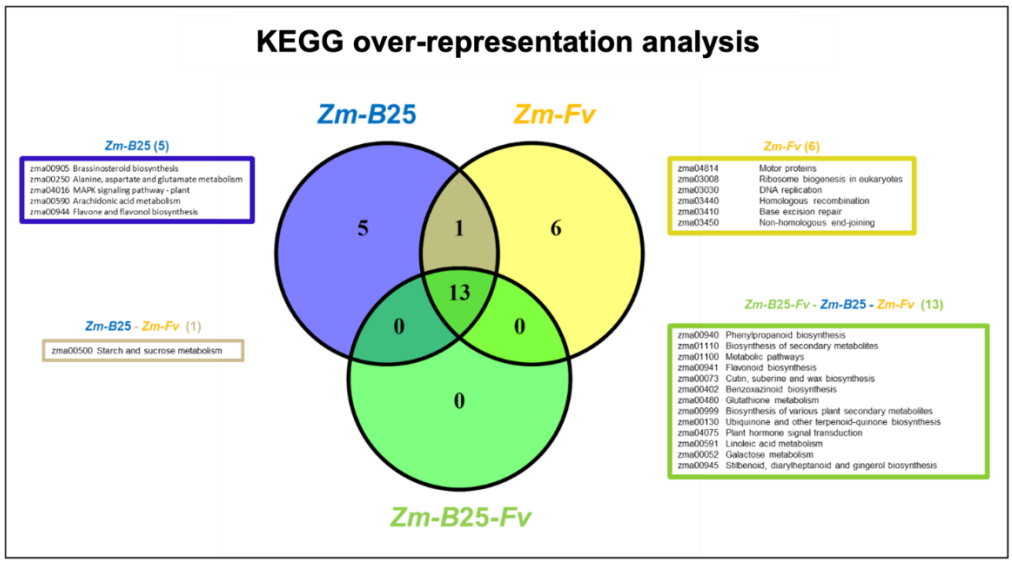

 doi:10.20944/preprints202510.2343.v1

Figure 4. Venn diagram of unique and shared overrepresented KEGG pathways between the interaction conditions. Boxes display the list of overrepresented KEGG terms exclusive to one or shared by two or three interactions.

The 13 KEGG overrepresented pathways common to all conditions were primarily linked to the biosynthesis of different secondary metabolites and the metabolism of glutathione, linoleic acid, and galactose. The starch and sucrose metabolism (zma00500) pathway was only altered when maize interacted with either *B*25 or *Fv* individually, but not when both microorganisms were present within the plant.

2.7. Functional Gene Association Networks: Enriched Biological PROCESSES using A. thaliana Orthologous Genes

Although the GO overrepresentation analysis based on maize gene annotations from BioMart provided insight into each interaction as described above, an additional GO enrichment analysis was conducted using *A. thaliana* orthologous genes (Supplementary methods, Supplementary Table 6) to examine the governing mechanisms behind each interaction. Using up- and downregulated genes from each interaction and intersection between them (Figure 2), we built gene network associations to understand the functional relationship among DEGs. Supplementary Table 7 shows the main results obtained from the analysis of NRGIs using String.

Analysis of NRGIs revealed the formation of diverse networks for each maize interaction (Supplementary Table 7). Even though the *Zm-B25-Fv*/*Zm-Fv*/*Zm-B25* (UP) gene set harbored the highest number of nodes (874), the *Zm-Fv* (DOWN) gene set (678) exhibited a higher number of edges (5866) than the former one (2560). Gene sets that produced a main network with fewer than 200 nodes were either expanded via String or submitted to Genemania as a complementary approach to identify enriched pathways. Significant associations for *Zm-B25-Fv* (UP), *Zm-B25-Fv*/*Zm-B25* (UP) and *Zm-B25-Fv*/*Zm-B25* (DOWN) were only detected after the String network expansion and Genemania analysis (Supplementary Table 7).

Overall, instead of evaluating individual genes, obtaining BPs from gene association networks allowed us to clearly and comprehensively identify the most prominent genes associated with each maize interaction (Figure 5). For all cases in which *Zm-Fv* appeared (4 out of 7; see sections *Zm-B25-Fv*/*Zm-Fv*/*Zm-B25*, *Zm-Fv*/*Zm-B25*, *Zm-Fv* and *Zm-B25-Fv*/*Zm-Fv*), the response to the stress-related stimulus (chemical) was the prevalent process among upregulated genes, whereas the process of DNA-related metabolism stood out among downregulated genes (Supplementary Table 7). Both processes covered 5473 DEGs (88.03%) out of the total 6217 DEGs. Even though the *Zm-B25-Fv*/*Zm-Fv*/*Zm-B25*, *Zm-Fv*/*Zm-B25*, *Zm-Fv* and *Zm-B25-Fv*/*Zm-Fv* interactions shared similar BPs within upregulated genes, *Zm-B25-Fv*/*Zm-Fv* exhibited exclusive BPs such as photosynthesis, generation of precursor metabolites and energy, and small molecule metabolic process, reinforcing the previous observation that *Zm-B25-Fv*/*Zm-Fv* differed slightly from the other interaction sections in which *Zm-Fv* was involved.

The remaining 744 DEGs (11.97%) clustered into the last three sections (*Zm-B25*, *Zm-B25-Fv* and *Zm-B25-Fv*/*Zm-B25*). BPs associated with upregulated genes were the most contrasting compared to 88.03% of DEGs. For example, *Zm-B25* harbored exclusive BPs such as carbohydrate metabolic process, cell wall organization or biogenesis, and regulation of macromolecule biosynthetic process, whereas *Zm-B25-Fv*/*Zm-B25* showed overrepresented processes such as phospholipid biosynthetic process and inositol metabolic process (Supplementary Table 7). On the other hand, *Zm-B25-Fv* featured BPs such as ribosome biogenesis, gene expression, rRNA processing, cellular nitrogen compound metabolic process, ribosome assembly, macromolecule metabolic process and translation. Finally, it is important to note that *Zm-B25* and *Zm-B25-Fv* also showed DNA-related metabolism processes among their downregulated genes, which differed sharply from *Zm-B25-Fv*/*Zm-B25* that featured BPs such as phosphatidylinositol-3-phosphate biosynthetic process, protein targeting mitochondrion, protein transmembrane transport, vacuole organization, photomorphogenesis and

 doi:10.20944/preprints202510.2343.v1

autophagy-related processes (Supplementary Table 7). Functional gene association networks therefore provide an overall insight into the transcriptomic behavior covering each section and intersection of maize interactions.

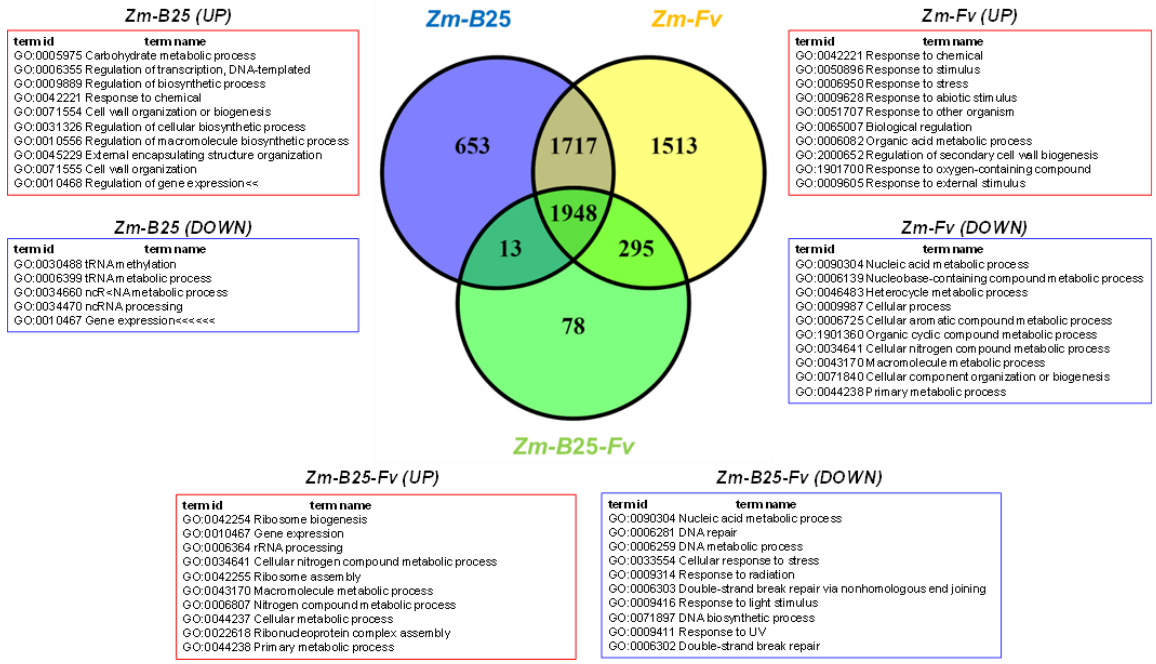

Figure 5. Enriched biological processes emerging after applying the Markov clustering (MCL) based on co-expression.

2.8. Gene Interaction Networks Based on Co-Expression

Gene associations often result in highly connected networks, with little informative power. Therefore, clustering them through algorithms allows for a better interpretation (Supplementary methods). The largest identified clusters turn out to be highly relevant to the main findings of the original network. Therefore, to gain more insight into previously described functional networks (Supplementary Table 7), Markov clustering (MCL) was performed based on co-expression using *A. thaliana* orthologs. Interactions involving *Zm-B25-Fv*, *Zm-B25* and *Zm-Fv*, as well as their corresponding intersections (*Zm-B25-Fv*/*Zm*-B25, *Zm-B25-Fv*/*Zm-Fv* and *Zm-B25*/*Zm-Fv*) were considered for this analysis.

The *Zm-B25*/*Zm-Fv* intersection harbored a main cluster among its upregulated genes related to stress response (response to chemicals and chitin) (Supplementary Table 7), cell wall remodeling (biosynthesis of secondary cell wall), phenylpropanoid metabolic process, oxoacid metabolic process, hormone-mediated signaling pathway (auxin) and photosynthesis. In *Zm-B25*, chromatin remodeling, gene expression, protein metabolic process (translation), nucleocytoplasmic trafficking of RNAs and proteins, phenylpropanoid-related metabolic process, hormone-mediated signaling pathway (auxin), protein phosphorylation (involved in growth and development), and thermotolerance were all exclusive to this interaction. BPs exclusive to the *Zm-Fv* interaction were found, such as response to external stimuli (bacteria and fungi), glycolysis, photosynthesis, carboxylic acid metabolic process (oxidative phosphorylation), very-long-chain fatty acid (VLCFA) biosynthesis, transition metal ion transport, pigment metabolic process, nitrate assimilation, cellular detoxification, proteasomal protein catabolic process, and circadian rhythm (Supplementary Table 7). Noteworthy, the cell wall biogenesis process, specifically the biosynthesis of secondary cell wall, was shared between *Zm-B25* and *Zm-Fv*.

Zm-B25-Fv exclusive BPs as well as BPs shared with *Zm-B25* and *Zm-Fv* were analyzed. First, upregulated *Zm-B25-Fv* genes exhibited overlapping BPs with *Zm-B25*, such as lipid metabolic

 doi:10.20944/preprints202510.2343.v1

processes (phospholipid biosynthetic process and inositol metabolic process), L-ascorbic acid biosynthetic process, transcription regulation of SA- (positive) and JA- (negative) related genes, and melatonin biosynthetic process. Secondly, the BPs shared with *Zm-Fv* included cellular response to oxidative stress (chemical), generation of precursor metabolites and energy (photosynthesis and glycolysis), cellular aldehyde metabolic process (related to oxidative stress tolerance), cellular detoxification, mRNA polyadenylation, VLCFA biosynthesis, and plant hormone signal transduction (ABA). Altogether, the above-described BPs allowed us to identify those exclusive BPs corresponding to *Zm-B25-Fv*, such as ribosome biogenesis (ribosome assembly), actin filament depolymerization and polysaccharide catabolic process (stress-induced starch degradation) (Supplementary Table 7). On the other hand, protein metabolic (translation) and lipid metabolic (phospholipid biosynthetic process) processes found in the *Zm-B25-Fv* interaction were also present in *Zm-B25* and *Zm-B25-Fv*/*Zm-B25*, respectively. However, it is important to note that the NRGIs involved in both BPs were not the same as between *Zm-B25-Fv* and *Zm-B25*, or between *Zm-B25-Fv* and *Zm-B25-Fv*/*Zm-B25*.

Although clusters formed by downregulated genes involved DNA metabolic processes in general, peculiarities of their interactions and intersections could be observed when compared to cluster-associated BPs of upregulated genes. For example, whereas *Zm-Fv* exhibited BPs associated with response to heat and protein folding in their downregulated genes, such BPs were among the upregulated *Zm-B25* genes. Furthermore, BPs associated with the process of translation (ribosome biogenesis, rRNA processing, and ncRNA metabolic process) identified among the downregulated genes of *Zm-Fv* and *Zm-B25* (as well as the *Zm-B25*/*Zm-Fv* intersection) were found among the upregulated genes of *Zm-B25-Fv*.

In addition to the identified exclusive BPs, other processes were also associated with the *Zm-B25-Fv* tripartite interaction, such as cellular response to oxidative stress and its corresponding counteracting mechanisms (transcription regulation of hormone-related genes [SA and JA], plant hormone signal transduction [ABA], cellular aldehyde metabolic process, and cellular detoxification involving the glutathione-ascorbic acid redox cycle). Changes occurring in the plasma membrane and plant cuticle are suggested by the identification of lipid metabolic processes (phospholipid biosynthetic process, inositol metabolic process and VLCFAs). Finally, the generation of precursor metabolites and energy (photosynthesis, glycolysis, and stress-induced starch degradation) also emerged as important processes occurring in this interaction. In summary, the *Zm-B25-Fv* interaction seems to harbor BPs related to plant growth and development (gene expression, RNA metabolic process, ribosome biogenesis, translation, actin filament depolymerization, photosynthesis and glycolysis), as well as BPs associated with plant protection triggered by pathogens (changes in plasma membrane and cuticle, as well as cellular response to oxidative stress), which may help explain the *B*25-mediated maize protection against *Fv*.

2.9. Validation of RNA Sequencing by qRT-PCR

To validate the RNA-seq data, eleven unique DEGs were selected based on their FC (high and/or low) from the interactions, and their expression profiles were evaluated by qRT-PCR. As indicated in Table 5, FC values obtained by qRT-PCR analysis displayed similar expression trends as in the RNA-seq data.

Table 5. Comparison of relative expression levels obtained by RNA-seq and qRT-PCR for selected genes from the unique DEGs of the interaction conditions.

Condition	ID[a]	Gene	Fold Change vs control	
			FC RNA-seq	FC qRT-PCR
*Zm-B*25-*Fv*	Zm00001eb375460	Glutaredoxin	11.49	4.11
	Zm00001eb229260	Protein kinase domain	2.18	2.24
	Zm00001eb251380	Cyclic nucleotide-binding domain	-2.23	-7.56

 doi:10.20944/preprints202510.2343.v1

	Zm00001eb029490	Gdt1 family	-2.41	-4.37
	Zm00001eb397080	CRAL/TRIO, N-terminal domain	-2.61	-2.74
*Zm-B*25	Zm00001eb124940	Multi antimicrobial extrusion protein	2.87	2.92
Zm-Fv	Zm00001eb041100	Hydroxycinnamoyltransferase 9	13.1	7.3
	Zm00001eb419890	Deoxymugineic acid synthase 6	5.09	5.57
	Zm00001eb285030	Putative cytochrome P450 superfamily protein	7.07	3.72
	Zm00001eb241870	Small auxin up RNA54	9.69	24.98

[a] Maize reference identifier (*Zea mays* B73 v5.0).

3. Discussion

Bacterial endophytes, which are abundant in plants, are currently being extensively studied due to their plant growth-promoting effect and their ability to protect plants against diseases. A deeper understanding of not only the bacterial endophyte-host plant interaction, but also the fungal pathogen-host plant interaction and the tripartite interaction between the bacterial endophyte, the fungal pathogen and the host plant can enhance the use of bacterial endophytes to overcome plant disease and improve agricultural production [15,16,24].

Previous studies have demonstrated the potential of *B*25 to protect maize plants against *Fv*, and to promote their growth at early [13,18] and late growth stages [9]. To better understand the molecular basis of the biocontrol and plant growth promotion induced by *B*25 on maize against the fungal pathogen *Fv*, we analyzed the transcriptomic changes of maize roots obtained at seven days after seed inoculation with *B*25 and *Fv*, either individually or combined. The expression patterns of a number of DEGs were validated (Table 5) in this work, complementary to a previous report in which ten induced maize chitinase DEGs were validated from the *Zm-Fv* condition [25]. To the best of our knowledge, this study represents the first report of a maize root transcriptome in response to the dual inoculation of two endophytes, i.e. a bacterial biocontrol agent and a fungal pathogen.

Plant-bacteria interaction (*Zm-B*25): *B*25 is recognized by maize as a beneficial microorganism

A core of 1,961 DEGs was shared among all conditions. Of these, only the gene *Zm00001eb141540* (geb1-glucan endo-1,3-beta-glucosidase homolog1), a β-1,3-glucanase, presented a contrasting pattern of expression in maize interacting with the different microorganisms (Supplementary Table 2). This gene was upregulated in the *Zm-B*25-*Fv* and *Zm-Fv* interactions, where *Fv* was present (Log2FC of 2.46 and 2.76, respectively), whereas it was downregulated in the *Zm-B*25 interaction (Log2FC of -2.93). Plant β-1,3-glucanases have a key role in plant–microbe interactions, and several β-1,3-glucanases are included in the pathogenesis related (PR) group 2 of proteins. This type of β-1,3-glucanase accumulates during a pathogen attack, and some of them have been directly involved in the hydrolysis of pathogen cell walls, since β-1,3-glucans are found in bacteria, metazoa, viruses, and particularly fungi [26]. Thus, the upregulation of *Zm00001eb141540* in maize roots in the presence of the fungus, and its downregulation when bacteria are present, could suggest that maize perceives the endophytic bacteria *B*25 as a non-threatening microorganism. Further analysis is necessary to demonstrate the role of *Zm00001eb141540* in the *Zm-B*25 association.

Moreover, overrepresented unique GO terms in *Zm-B*25 were related to the establishment of a beneficial plant-bacteria interaction (Figure 3), including carbohydrate metabolic processes (GO:0005975), oligopeptide transport (GO:0006857), and phenylpropanoid metabolic processes (GO:0009698); these compounds have been reported as chemo attractants in plant roots (Villarino et al., 2021). Plant roots can secrete organic exudates into their surroundings, which attract beneficial microorganisms, establishing a favorable plant-bacteria interaction (Sasse et al., 2018). Furthermore, the GO term calcium-dependent phospholipase A2 activity (GO:0047498) was exclusively overrepresented in *Zm-B*25. A key process in the beneficial plant-bacteria interaction is the increase in calcium flow and reactive oxygen species, leading to lipid oxidation in the cell membrane, indicating a favorable relationship (Gowtham et al., 2022). The GO term lipid oxidation (GO:0034440)

 doi:10.20944/preprints202510.2343.v1

appeared between the overrepresented GO terms in *Zm-B*25, but also in *Zm-Fv*. Quercetin 3-O-glucosyltransferase (GO:0080043) and quercetin 7-O-glucosyltransferase (GO:0080044) activities appeared as overrepresented GO terms only in those interactions where *B*25 was present (*Zm-B*25 and *Zm-B*25-*Fv*) (Figure 3). Quercetin is a flavonol from the flavonoid subclass that is linked to the establishment of plant interactions with other beneficial organisms, including the arbuscular mycorrhizal association and the symbiosis between legumes and nitrogen-fixing rhizobia (Singh et al., 2021; Zhang et al., 2013). Flavonoids also work as communication mediators between PGPRs and plants, suggesting that they might play a key role in these interactions (Wang et al., 2022). Taking these biological processes together may help to explain how maize plants perceive the *B*25 bacterium as a beneficial microorganism.

Plant-bacteria interaction (Zm-B25): *B*25 induces the activation of pathways related to plant growth, development, and the defense response

Our study revealed the induction of several unique KEGG pathways during the interaction between maize and *B*25 (*Zm-B*25) at 7 dpi. These pathways, mainly related to plant growth and development and defense responses, include brassinosteroid biosynthesis; alanine, aspartate and glutamate metabolism; flavone/flavonol biosynthesis; plant MAPK signaling pathway; and arachidonic acid metabolism.

Zhang et al., (2022) showed that the exogenous addition of brassinosteroids (BRs) to maize promotes root growth, enhances stress tolerance, and increases grain yield. Specifically, root development was attributed to the regulation of BRs via auxin, implicating the upregulation of the *ZmWOX5*, *ZmBBM1* and *ZmBBM2* homologs of *PLT1* and *PLT2*, as well as the auxin transporter genes *ZmPIN2*, *ZmPIN3a* and *ZmPIN3b* and the positive auxin response factors (ARF) that promote the initiation of lateral root primordia in *ZmARF7* and *ZmARF19*. None of these genes were induced within the unique DEGs in *Zm-B*25; instead, *Zm00001eb433020* (arftf29-ARF-transcription factor 29) was downregulated (Log2FC= -1.55), and *Zm00001eb026490* (aic1-auxin import carrier1) was upregulated (Log2FC= 1.23). Nonetheless, four genes related to auxin response were identified within the unique EGs in *Zm-B*25: *Zm00001eb321090* (saur66 - small auxin up RNA66), *Zm00001eb070660* (saur17 - small auxin up RNA17), *Zm00001eb321100* (saur67 - small auxin up RNA67), and *Zm00001eb218080* (umc2293 - auxin responsive protein). These four genes belong to the small auxin-up RNA (*SAUR*) gene family, which itself forms part of three different early auxin-responsive gene families [31]. *SAUR* genes are involved in the auxin signaling pathway, and their expression can be induced within 2–5 min by active auxin [31,32]. These observations suggest that the expression of *SAUR* genes mediated by *B*25 could play a key role in the regulation of BRs, to promote maize growth.

Amino acids play vital roles in the central metabolism of plants, as they are involved in physiological processes that are directly or indirectly linked to the synthesis of diverse metabolites [33]. Amino acids and their derivatives have prominent functions in plants, such as protein synthesis, growth and development, nutrition, and stress responses (Hildebrandt et al., 2015). Among other amino acids, glutamate, aspartate, and alanine are used in the formulation of biostimulants [34]. Alfosea-Simón et al., 2021 studied the effects of exogenous applications of these three amino acids on tomato growth, and found a positive effect of aspartic and glutamic acid on plant growth. Foliar application of glutamine (Gln) at the V6, V8, V12, R1 (silk), and R3 (dough) stages in maize hybrid ZD958 impacts grain yield and nutritional quality, enhancing grain yield by 20% under sufficient N, and by 38% under low N (Slam et al., 2024). In this work, non-significant differences at an early stage of maize development (7 dpi) were observed between *Zm-B*25 and the control condition (*Zm*), related to the evaluated growth parameters (Table 1). This is possibly due to the developmental stage of the evaluated plantlets. Nonetheless, previous field work demonstrated that maize inoculation with the biocontrol agent *B*25 significantly increased plant growth and grain yield in several field sites and crop seasons, compared to untreated (*Zm*) and *Fv*-inoculated controls (*Zm-Fv*) [9]. *B*25 may induce the activation of glutamate, aspartate and alanine metabolic pathways as a key mechanism in maize to promote growth and increase grain yield. It is possible that *B*25-mediated induction of amino acid metabolism at an early growth stage (7 dpi) remains induced at later maize developmental stages,

 doi:10.20944/preprints202510.2343.v1

but further maize transcriptome analysis at later developmental stages will be necessary to confirm this hypothesis.

Mitogen-activated protein kinases (MAPKs) play essential roles in plant growth and development by regulating both cell differentiation and proliferation [37]. MAPKs are also important signaling modules in eukaryotes, with key roles in regulating responses to four major environmental stresses (high salinity, drought, extreme temperature, and insect/pathogen infections) via gene expression regulation, plant hormone production, and crosstalk between environmental stresses (Lin et al., 2021). In the *Zm-B*25 interaction, 29 DEGs were found in the overrepresented MAPK plant signaling pathway, with most of them related to stress adaptation, defense response, pathogen defense and late pathogen defense response (data not shown). All of these DEGs were upregulated, except for *Zm00001eb133330* (Mitogen-activated protein kinase kinase 3).

In addition to the MAPK plant signaling pathway, arachidonic acid metabolism also appeared as an overrepresented KEGG pathway in the *Zm-B*25 interaction, with five upregulated DEGs. Arachidonic acid (AA) is an evolutionarily conserved signaling molecule that modulates plant stress signaling networks, and which acts as an elicitor of pathogen defense response and plant programmed cell death [39,40]. Dye & Bostock, (2021) demonstrated that the exogenous addition of AA to the roots of tomato and pepper seedlings protects them against root and crown rot caused by *Phytophtora capsici*. Lewis et al., (2023) showed that tomato roots treated with AA altered the tomato metabolome with an enrichment of chemical classes and the accumulation of metabolites associated with defense-related secondary metabolism. Among the five upregulated DEGs found in this overrepresented KEGG pathway, *Zm00001eb184300* ((+)-neomenthol dehydrogenase) was the second-most upregulated gene (log2FC= 3.2). The menthone reductase gene *CaMNR1* in *Capsicum annuum* and its ortholog *AtSDR1* in *Arabidopsis thaliana* were observed to positively regulate plant defenses against a broad spectrum of pathogens. Specifically, *CaMNR1*-overexpressing *Arabidopsis* plants exhibited enhanced resistance to the hemibiotrophic pathogen *Pseudomonas syringae* pv. *tomato* DC3000 and the biotrophic pathogen *Hyaloperonospora parasitica* isolate Noco2, whereas a mutation in *AtSDR1* significantly enhanced susceptibility to both pathogens [43]. This suggests that the maize gene *Zm00001eb184300* in the *Zm-B*25 interaction could be implicated in preparing plant defense responses against pathogen attack.

The induction of flavone/flavonol biosynthesis detected by KEGG analysis in the *Zm-B*25 interaction could contribute to plant growth and development as well as the defense response, as this plant-specialized secondary metabolite performs many functions in plants, including plant color development, cell growth regulation, attraction to pollinators, and protection against biotic and abiotic stresses (Alseekh et al., 2020; Dias et al., 2021; Wang et al., 2021).

Some other unique GO terms significantly overrepresented in *Zm-B*25 were related to plant defense and growth promotion. These include the cinnamic acid biosynthetic process (GO:0009800), which is involved in the biosynthesis of secondary metabolites related to plant defense and acts as an antioxidant, promoting plant growth (Jiménez-Gómez et al., 2020); the plant-type secondary cell wall biogenesis (GO:0009834); and plant-type cell wall organization (GO:0009664). The last two GO terms may contribute to optimal cell wall development and the providing of mechanical resistance (Dauwe et al., 2007). *Zm00001eb399600* (allene oxide synthase, *aos1*) was a unique upregulated DEG (Log2FC of 2.09) in *Zm-B*25. This defense-related gene is overexpressed in maize plants when they come into contact with the PGPR *Klebsiella jilinsis* (Zhang et al., 2021).

Plant-pathogenic fungus interaction (*Zm-Fv*): *Fv* turns off DNA replication and repair, and negatively affects plant growth and development

The genomic integrity of every organism is constantly challenged by endogenous and exogenous DNA-damaging factors, and maintaining this integrity is crucial to the proper development of all living organisms and the faithful transmission of genetic information from one generation to the next [47,48]. The most important sources of DNA damage are endogenous, including oxidative metabolism, spontaneous hydrolytic reactions, and replication machinery errors, although environmental factors such as ionizing and UV radiation, and genotoxic biogenic or industrial

 doi:10.20944/preprints202510.2343.v1

chemicals, also contribute significantly [49]. Because plants are attached to their substrate, they cannot avoid these stresses. Therefore, proper sensing of DNA damage and the precise activation and functioning of the DNA repair machinery is of foremost importance in preserving genome integrity [50]. In the present work, our results highlight that the main effect of *Fv* in maize roots is the downregulation of genes related to DNA replication and maintenance. Both KEGG and GO enrichment analyses (Figures 3 and 4) confirmed the enrichment of unique pathways (motor proteins, ribosome biogenesis in eukaryotes, DNA replication, homologous recombination, base excision repair, and non-homologous end-joining) and GO terms (DNA binding, transmembrane transporter activity, single-stranded DNA helicase activity, DNA replication initiation, and negative regulation of DNA recombination) associated with DNA replication and repair processes. Co-expression network analysis further supports this observation, as it revealed DNA replication and maintenance within the modules with downregulated, significantly enriched terms only in the *Zm-Fv* condition (Supplementary Tables 6 and 7). Moreover, an independent GO analysis assessing the unique downregulated DEGs (809 out of 1,513 DEGs) in this condition confirmed the overrepresentation of the following GO terms related to DNA metabolism: organelle organization, chromosome organization, DNA metabolic, nucleic acid metabolic process, and cellular component organization or biogenesis (Supplementary Table 7).

One key mechanism of DNA repair processes is the DNA Damage Response (DDR). This mechanism activates the DNA repair pathways BER (base excision repair), NER (nucleotide excision repair), and MMR (mismatch repair mechanism) for single-strand breaks, as well as HR (Repair–Homologous Recombination) and NHEJ (Non-Homologous End Joining) for double-strand breaks (DSB) [48–50]. We observed that both single-strand and double-strand DNA repair processes were affected by *Fv* in maize roots in the *Zm-Fv* condition. Five DEGs associated with the Non-Homologous End Joining Pathway were downregulated: *Zm00001eb116810* (ATP-dependent DNA helicase 2 subunit KU70), *Zm00001eb371940* (DNA polymerase lambda (POLL)), *Zm00001eb181120* (DNA repair protein RAD50), *Zm00001eb069270* (double-strand break repair protein MRE11), and *Zm00001eb071490* (putative DNA ligase 4). Similarly, a total of 18 DEGs in the Homologous Recombination Pathway were also downregulated, including genes coding for DNA polymerase I A (Zm00001eb431790) and delta (*Zm00001eb201340* and *Zm00001eb002170*), DNA repair proteins (*Zm00001eb255780* and *Zm00001eb181120*), and DNA topoisomerases (*Zm00001eb005010* and *Zm00001eb317420*), as well as 17 DEGs in the DNA Replication Pathway.

Fv affected maize root growth and development by turning off the pathways of ribosome biogenesis and motor proteins (Figure 4). From a total of 31 DEGs related to the ribosome biogenesis pathway in the *Zm-Fv* condition, only *Zm00001eb332570* (eukaryotic translation initiation factor 6) appeared as upregulated, while the rest were downregulated. Given the central function of ribosomes as the molecular machines responsible for protein synthesis, ribosome biogenesis is tightly linked with plant growth and development [51] and thus also the correct development of plant roots. Moreover, DEGs coding for kinesin (1 DEG), kinesin like-protein (11) and kinesin-related protein (4) were downregulated, along with two myosin-17 genes. Kinesins and myosins are motor proteins that can move actively along microtubules and actin filaments, respectively, coordinating diverse cellular functions in plants [52]. Kinesins are responsible for unidirectionally transporting various cargos, including membranous organelles, protein complexes, and mRNAs; they also play critical roles in mitosis, morphogenesis, and signal transduction, and contribute directly or indirectly to cell division and cell growth in various tissues (Li et al., 2012). In contrast, myosin drives cytoplasmic streaming, actin organization, and cell expansion, thus performing supporting roles in plant growth, environmental responses, and the defense against pathogens[54].

The tripartite interaction *Zm-B*25-*Fv*: induction of defense response genes and plant growth development

A common molecular response was found to be derived from the interactions of maize roots with 1) *B*25 (*Zm-B*25); 2) *Fv* (*Zm-Fv*); and 3) both microorganisms (*Zm-B*25-*Fv*). This response included 22,576 core EGs (Figure 1), 1,948 core DEGs (Figure 2), 42 core overrepresented GO terms (Figure 3,

 doi:10.20944/preprints202510.2343.v1

Supplementary Table 4), and 13 core overrepresented KEGG pathways (Figure 4). In contrast, a differential and unique response was observed for each interaction, which was stronger when microorganisms interacted separately with maize than at the same time (i.e. the tripartite interaction).

The *Zm-B*25-*Fv* tripartite interaction did not present any unique overrepresented KEGG pathways (Figure 4) that could explain the molecular mechanisms involved in the plant response during this interaction, aside from a few unique overrepresented GO terms and unique DEGs. From a total of 78 unique DEGs in *Zm-B*25-*Fv*, 34 of them were upregulated and 44 were downregulated. The top ten upregulated DEGs include four genes that are directly and/or indirectly (orthologous genes) involved in plant resistance against different pathogens. These four genes are *Zm00001eb282040* (glp1 - germin-like protein1; log2FC= 4.37); *Zm00001eb339590* (ABC transporter G family member 34; log2FC= 3.87), the most induced DEG; *Zm00001eb393680* (peroxidase 5; log2FC= 3.18); and *Zm00001eb009380* (LysM-containing Receptor-Like Kinases LYK2; logFC=2.22).

When overexpressed in *Arabidopsis*, *Zm00001eb282040* (glp1) improves the resistance to the biotrophic *P. syringae* pv. tomato DC3000 (*Pst*DC3000) and the necrotrophic *Sclerotinia sclerotiorum* pathogens by inducing the expression of JA signaling-related genes [55]. In support of this, the GO term response to jasmonic acid (GO:0009753) was only found as an overrepresented GO term in the *Zm-B*25-*Fv* interaction (Figure 3). *AtABCG34*, the *Arabidopsis* ortholog of *Zm00001eb339590* (ABC transporter G family member 34 [LOC103635032]), mediates camalexin secretion to defend against the necrotrophic pathogens *Alternaria brassicicola* and *Botrytis cinerea* [56]. Compared to the susceptible maize inbred line PH4CV, the resistant inbred maize line 9D207 exhibits significantly induced expression of the phenylpropanoid biosynthesis-related genes *Zm00001eb393680* (peroxidase 5 [LOC103639086]), *Zm00001eb381290* (peroxidase), *Zm00001eb225390* (*EC 3.2.1.21*), *Zm00001eb318150*, *Zm00001eb329520* (*bglB*), *Zm00001eb160830* (*REF1*) and *Zm00001eb158880* (*TOGT1*) when infected by spray-inoculation of an *Exserohilum turcicum* spore suspension (Li et al., 2024). This suggests a possible plant defense role for these phenylpropanoid biosynthesis-related genes. Finally, gene *Zm00001eb009380* ([LOC103633076] Protein LYK2) is a member of the LysM-containing Receptor-Like Kinases (LYKs), which play a key role in the plant defense response. LysM and LYK proteins are the second major class of plant recognition receptors (PRPs) after LRR-RPs/LRR-RLKs, playing a significant role in the plant immune response [58]. In *A. thaliana,* LYK2 proved to be dispensable for chitin perception and early signaling events, but necessary for enhanced resistance to *B. cinerea* and *P. syringae* induced by flagellin, and for elicitor-induced priming of defense gene expression during fungal infection. LYK2 overexpression in *Arabidopsis* enhances resistance to *B. cinerea* and *P. syringae* and results in increased expression of defense-related genes during fungal infection (Giovannoni et al., 2021). Thus, due to the crucial role of LYK2 in *Arabidopsis* for chitin perception, it is possible that Zm00001eb009380 is essential for *Fv* detection, since chitin is a major component of the fungal cell wall (Elieh-Ali-Komi et al., 2016).

Other defense response-related genes were found among the *Zm-B*25-*Fv* unique upregulated DEGs, including *Zm00001eb371160* (pme39 - pectin methylesterase39), *Zm00001eb415440* (indole-2-monooxygenase-like [LOC103641249]), *Zm00001eb001120* (ATPP2-A13 [LOC100286177]), and *Zm00001eb259950* (NDR1/HIN1-like protein 1 [LOC100284275]). Gene *Zm00001eb371160* (pme39) is a member of the pectin methylesterases (PMEs), which modify pectin, a complex polysaccharide constituent of plant cell walls. PMEs are implicated in various biological processes, including fruit ripening, pathogen defense, and cell wall remodeling [60]. In *A. thaliana*, AtPME17 activity triggers the synthesis of plant defensin 1.2 (PDF1.2) through the jasmonic acid-ethylene signaling pathway, conferring resistance to the fungal pathogen *B. cinerea*, while in wheat, the expression of several PME genes was associated with resistance to *F. graminearum*, the causal agent of head blight [60].

Zm00001eb415440, an indole-2-monooxygenase-like gene, is involved in the biosynthesis of benzoxazinoids, which are protective and allelopathic compounds found in some plants such as maize, wheat, rye and other wild and cultivated Poaceae. Benzoxazinoids have been associated with biochemical defense against a variety of biotic stresses, including insect herbivory, microbial pathogens, and competition with other plant species (Zhou et al., 2018).

 doi:10.20944/preprints202510.2343.v1

The *A. thaliana* AtPP2-A1 gene ortholog of the maize *Zm00001eb001120* (ATPP2-A13) gene exhibits molecular chaperone and antifungal activities against *F. moniliforme*, *F. solani*, *Rhizoctonia solani* and *Trichoderma harzianum* [62]. Overexpressing AtPP2-A1 in *A. thaliana* inhibited the phloem-feeding behavior of the aphid *Myzus persicae*, indicating a potential role for PP2 genes in mediating plant defense against insect herbivory [63]. Finally, the gene *Zm00001eb259950* (NDR1/HIN1-like protein 1) is a member of the NHL protein family, involved in plant resistance to biotic and abiotic stresses. In the *Arabidopsis* genome, 45 NHL (NDR1/HIN1-like) genes that are homologous to NDR1 (non-race-specific disease resistance) or HIN1 (harpin-induced) genes have been identified, and their functions in pathogen perception have been extensively studied. Overexpression of NHL2 in *Arabidopsis* induced the expression of PR1 (pathogenesis-related gene 1) and light-dependent 'speck disease-like' symptoms in the leaves of transgenic plants. Likewise, overexpression of NHL3 increased resistance to *P. syringae* pv. tomato DC3000 [64]. Moreover, the overexpression of the *A. thaliana* genes NHL1 and NHL8 in soybeans enhanced resistance to the pathogen *Heterodera glycines* by activating the jasmonic acid (JA) and ethylene (ET) pathways [65].

Other upregulated unique DEGs found in the *Zm-B*25-*Fv* tripartite interaction relevant to plant defense are: *Zm00001eb153350*, a receptor-like protein 51 (*LRR6*) that can recognize microbial proteins or peptides [66]; *Zm00001eb426640* (nactf65 - NAC-transcription factor 65), which is part of the NAC transcription factor family and plays crucial regulatory roles in plant immunity [67]; *Zm00001eb249860*, an actin depolymerizing factor (*adf13*) involved in actin dynamics [68]; *Zm00001eb333050* (α-xylosidase 1 [LOC107548101]), an α-xylosidase that participates in remodeling xyloglucan, involved in the mechanical integrity of the primary cell wall of growing tissues, cell expansion, and seed germination (Shigeyama et al., 2016); and *Zm00001eb072230*, an S-norcoclaurine synthase 2. Norcoclaurine synthase (NCS) from *Thalictrum flavum* (Tf NCS), *Papaver somniferum* (Ps NCS1 and Ps NCS2), and *Coptis japonica* (Cj PR10A) share substantial identity with pathogen-related 10 (PR10) and Bet v1 proteins [62]. In support of the possible function of these unique upregulated DEGs, the term defense response (GO:0006952) was only found in the *Zm-B*25-*Fv* interaction as an overrepresented GO-term.

On the other hand, genes *Zm00001eb102960* (Log2FC= -3.37) and *Zm00001eb311640* (Log2FC= -3.64) were found as annotated genes within the top ten most downregulated DEGs. *Zm00001eb311640* is an elongation factor 2 protein that helps ribosomes move along messenger RNA during protein synthesis (White-Gilbertson et al., 2008);, while *Zm00001eb102960* is an SH3 domain-containing protein 3. Overexpression of SH3P2 in rice variety japonica YY compromised Pib-mediated resistance to *M. oryzae* isolates carrying AvrPib and Pib-AvrPib recognition-induced cell death [71]. Regarding the remaining downregulated DEGs, the genes *Zm00001eb296580* (GTP-binding nuclear protein Ran-2), *Zm00001eb156510* (9DNA ligase 6), *Zm00001eb341090* (parp1 - poly(ADP-ribose) polymerase1), *Zm00001eb029490* (TFIID basal transcription factor complex) and *Zm00001eb226110* (DNA repair protein REV1) were related to synthesis and/or DNA repair and transcription. The genes *Zm00001eb101530* (probable galacturonosyl-transferase 4), *Zm00001eb325370* (pdcb44 - plasmodesmata callose binding protein44) and *Zm00001eb336480* (rhamnogalacturonan I rhamnosyl-transferase 1) were related to the plant cell wall. The genes *Zm00001eb230490* (mate6 - multidrug and toxic compound extrusion6), *Zm00001eb293110* (trps12 - trehalose-6-phosphate synthase12), *Zm00001eb251380* (jmj15 - JUMONJI-transcription factor 15), *Zm00001eb332340* (mybr2 - MYB-related-transcription factor 2), *Zm00001eb182690* (prh37 - protein phosphatase homolog37) and *Zm00001eb154830* (type I inositol 1,4,5-trisphosphate 5-phosphatase 1-like) were reported to be associated with salinity, drought, chilling and cold stress. Finally, *Zm00001eb395630* (gpdh3 - glucose-6-phosphate dehydrogenase3) was associated with ROS homeostasis; *Zm00001eb203230* (naat1 - nicotianamine aminotransferase1) with iron (Fe) acquisition; and *Zm00001eb151610* (inositol-hexakisphosphate kinase/IP6K) with plant defense mechanisms against bacterial, fungal and viral infections. Overall, despite a considerable number of unique downregulated DEGs related to different mechanisms relevant to maize growth and development, no DEGs stood out in the tripartite interaction. Nevertheless, extended gene network analysis (Supplementary Table 7) shows that

 doi:10.20944/preprints202510.2343.v1

biological processes involved in plant growth and development such as gene expression, RNA metabolic process, ribosome biogenesis, translation, actin filament depolymerization, photosynthesis and glycolysis may be relevant to the tripartite interaction. This is in agreement with observations in this work and in the field where maize seed inoculation with *B*25 results in a growth response and even an increased grain production (Lizárraga-Sánchez et al., 2015). Together, the gene interaction network results based on co-expression, using *A. thaliana* orthologous genes and focusing on BPs, support the GO and KEGG findings, as addressed in this Discussion section.

The present work reveals molecular mechanisms used by maize when interacting simultaneously with two quite different microbes: a beneficial bacterium and a fungal pathogen. However, a complete understanding of the molecular mechanisms triggered by microbial inoculation in plants will require more research devoted to understanding the tripartite interaction, as well as the more complex plant-microbe interactions in the rhizosphere.

4. Materials and Methods

4.1. Microorganisms and Inoculum Preparation

The biocontrol maize endophyte *Bacillus cereus sensu lato* strain *B*25, isolated from the rhizosphere [13] and the maize pathogenic fungus *Fusarium verticillioides* strain P03, isolated from maize roots [4] were used in this study. Both microorganisms are kept as cryopreserved frozen stocks (-70 °C) at the CIIDIR-IPN Sinaloa Unit. For bacterial inoculum, a powder formulation based on *B*25 spores obtained according to Martínez-Álvarez et al., (2016) was used. The fungal inoculum *Fv* P03 was reactivated from a frozen stock by growing it on PDA plates at 25 °C for 10 days. *Fv* conidia were harvested using sterile distilled water and adjusted to a concentration of 1 x 10^6 conidia mL^{-1}. Harvested conidia were used as fungal inoculum.

4.2. Tripartite Assay: Maize-Bacteria-Fungus Interaction

Four conditions were established in this experiment: 1) maize without microorganisms (*Zm*), as a control; 2) maize inoculated with *B*25 (*Zm-B*25); 3) maize inoculated with *Fv* (*Zm-Fv*); and 4) maize inoculated with both *B25* and *Fv* (*Zm-B*25-*Fv*). Commercial maize seeds (Garañón hybrid, Asgrow) were surface-disinfected using a hydrothermal treatment [4]. Subsequently, seeds were immersed in a Tween-20 solution (5 drops of Tween-20 per 100 mL of sterile distilled water) and sonicated for 5 min. The Tween solution was then decanted, and seeds were immersed in a 0.75% sodium hypochlorite solution and placed in a thermal bath at 52 °C for 20 min. Finally, the seeds were washed three times with sterile distilled water and allowed to air dry in a laminar flow hood.

For *Zm-B*25 and *Zm-B*25-*Fv* conditions, disinfected maize seeds were inoculated with *B*25 powder formulation as in Martínez-Álvarez et al., (2016). Seeds were moistened with 0.4 mL of 1% CMC (w/v) and then coated with 2 g of powder formulation (1 x 10^9 spores mL^{-1}). The mixture was then stirred until the formulation completely covered the seeds, and the excess formulation was removed. The final inoculum concentration was 1 x 10^6 CFU of formulated *B*25 spores per seed. For *Zm* and *Zm-Fv* conditions, the seeds were coated with the same powder formulation but without *B*25 spores.

The rolled paper towel technique (Warham et al., 1996) was used with modifications to assay the interaction of maize with the microorganisms. Four pieces (1 cm^2) of sterile filter paper were placed on a 36 x 19.5 cm sterile paper towel previously moistened with sterile distilled water. For *Zm-Fv* and *Zm-B*25-*Fv* conditions, the sterile filter papers were inoculated with 1 x 10^4 *Fv* conidia, whereas for the *Zm* and *Zm-B*25 conditions, the sterile filter papers were inoculated with sterile distilled water. A single maize seed was placed on each of the four sterile filter papers (four seeds per paper towel), and the paper towel was rolled and maintained in sterile plastic bags. Each plastic bag contained three rolls (12 seeds in total) and represented one biological replicate for the fungal biocontrol and plant growth assays. Three plastic bags with three rolls each were placed in an acrylic sterile box and sealed with Micropore tape (3M™ Micropore™ surgical tape 1530-1) to avoid possible contamination.

 doi:10.20944/preprints202510.2343.v1

Acrylic boxes were then placed in a growth chamber at 28 °C, 60% relative humidity (RH), and a 16:8 h (light:darkness) photoperiod for seven days. Acrylic boxes were opened once per day in a laminar flow hood to remove excess humidity inside the boxes, and to moisten the rolled paper towels with sterile distilled water as needed. Subsequently, the boxes were resealed with micropore tape.

4.3. Maize Root Colonization and Plant Protection Mediated by B25 Against Fv

To confirm the protective effect of *B*25 on maize plants against *Fv* and the colonization of maize roots by both microorganisms during the tripartite assay, growth parameters were evaluated in five plants. Superficially disinfected root pieces were then used to re-isolate the microorganisms on LB and PD agar plates. Immediately after harvesting the five plants, fresh weight and shoot and root length were measured using an analytical balance (HR-150AZ, A&D Company, Tokyo, Japan) and a graduated ruler, respectively. Later, roots were superficially disinfected as in Jasim et al., (2014) with modifications. Roots were washed with tap water and cut into 1-2-cm long pieces. Root pieces were submerged in 70% ethanol for 1 min and in 1% sodium hypochlorite for 10 min. Next, the samples were dipped into a 10% (v/v) Tween-20 solution (Sigma, Cat. P7949) for 1 min and then washed three times with sterile distilled water. Disinfected root pieces were air-dried in a laminar flow hood, longitudinally cut, and placed on LB and PD agar plates, and finally incubated at 30 °C for 24-48 h.

4.4. RNA Extraction and Sequencing

Five out of twelve maize plants from a single bag were randomly selected. Entire root systems were pooled, immediately frozen in liquid nitrogen, and subsequently ground using a sterile pestle and mortar. The root pool from the five plants was used as a biological replicate for RNA extractions. The total RNA of three biological replicates was extracted using TRIzol® reagent (Thermo Fisher Scientific, Cat. No. 15596-026, Waltham, MA). The concentration and quality (260/280 nm ratio) of the total RNA were estimated by spectrophotometry using a Nanodrop 2000c (Thermo Fisher Scientific, Wilmington, DE), and RNA integrity was determined by agarose gel electrophoresis [73]. RNA samples were sent to the Genomic Services Laboratory (LabServGen CINVESTAV-IPN Irapuato, México) for sequencing. Before processing, the RNA integrity number (RIN) was verified using the Agilent RNA 6000 Nano Kit. All samples presented an RIN value >7. Twelve independent libraries, corresponding to three biological replicates from each condition (*Zm*, *Zm-B*25, *Zm-Fv*, and *Zm-B*25-*Fv*) were constructed using the Illumina® TruSeq RNA sample prep v2 kit. Libraries were sequenced in paired-end format (2x150 bp) in the Illumina NextSeq 500 platform.

4.5. Bioinformatic Analysis

Bioinformatic analyses were performed using the OOREAM computing server at the CIIDIR-IPN Sinaloa Unit. The quality of reads was examined before and after the trimming process with FastQC v0.11.4 (https://www.bioinformatics.babraham.ac.uk/projects/fastqc). Raw reads were filtered using Trimmomatic v0.39 [74] with a minimum quality score of 20 and a minimum length of 50 bp. Illumina adapters were also removed during this step. Trimmed reads were mapped to the reference genome of *Zea mays* B73 v5.0 [75] using the STAR v2.7.0 software [76] with default parameters. Gene expression levels of SAM files were estimated based on the number of uniquely mapped reads using the HTSeq-count v0.11.1 software [77]. Raw counts were imported into the R/DESeq2 v1.32 package [78] for differential expression analysis. For principal component analysis (PCA), raw counts from all 12 libraries (4 conditions with 3 replicates) were normalized using the variance-stabilizing transformation (vst) method. One atypical replicate per condition was identified and removed for further analysis. The remaining 8 libraries (4 conditions with 2 replicates) were then normalized using the median of ratios method to identify differentially expressed genes (DEGs) between two selected conditions. DEGs were defined as genes with an adjusted *P*-value <0.01 and |Log2 fold change| >1. The interaction conditions *Zm-B*25, *Zm-Fv* and *Zm-B*25-*Fv* were individually compared against the control *Zm* to obtain a total of three sets of DEGs, corresponding to each

 doi:10.20944/preprints202510.2343.v1

comparison. Next, DEGs from the three interaction conditions (*Zm-B*25, *Zm-Fv* and *Zm-B*25-*Fv*) were compared in a Venn diagram to identify unique and common DEGs among them.

4.6. Gene Function Annotation and Overrepresentation Analysis

Gene ontology (GO) terms were obtained from the Ensembl database [79] using the BioMart tool (https://plants.ensembl.org/biomart/) and assigned to the DEGs of the three interaction conditions. Next, DEGs of each interaction condition were subjected to GO and KEGG overrepresentation analyses independently.

GO overrepresentation analysis was performed using the R/goseq v1.44 package [80] with the Wallenius method. GO terms with an adjusted *p*-value <0.05 were considered as significantly overrepresented.

KEGG overrepresentation analysis was performed in the Database for Annotation, Visualization and Integrated Discovery (DAVID) (https://david.ncifcrf.gov/). The DEG lists were loaded into the database and gene identifiers were linked to ENSEMBL_GEN_ID. KEGG pathways with an adjusted p-value <0.05 were considered as significantly overrepresented.

4.7. Gene Set Enrichment Analyses: Networks and Clustering

To investigate whether the set of genes from each section and intersection of maize interactions were associated with certain biological pathways, non-redundant gene identifiers (NRGIs) from *A. thaliana* orthologous genes corresponding to up- and downregulated maize genes were submitted to AgriGO [81], as well as to String [82] and Genemania [83]. The functional enrichment analyses generated GO terms belonging to biological processes (BPs), molecular functions (MFs), and cellular components (CCs). The most significant GO terms and pathways were those with an FDR threshold of 5% and a redundancy score set at 0.5. In the case of network analysis, all gene sets that generated a main network containing less than 200 nodes were expanded via String. Moreover, the same former gene sets were also submitted to Genemania as a complementary approach to identify enriched pathways. For network clustering based on co-expression, the Markov clustering (MCL) method of StringApp was employed with an inflation value set to 2.5 and STRING interaction scores of 0.4. Only the largest clusters were further used for functional enrichment analysis. Network associations were visualized and analyzed in Cytoscape v3.9.1 [84].

4.8. RNA-Seq Validation by qRT-PCR

Quantitative RT-PCR experiments were carried out on the same RNA samples used for RNA-seq. Total RNA was DNase treated (RQ1 DNase). First-strand cDNA was synthesized from 1 µg of total RNA using SuperScript III reverse transcriptase (Thermo Fisher Scientific, Cat. No.18080-044, Waltham, MA) following the manufacturer's instructions. qRT-PCR reactions were conducted in a Rotor Gene-Q Real time PCR system (Qiagen, Cat. No. 9001550, Hilden, Germany); four technical replicates were performed for each of the two biological replicates. Reactions included 5 µL of SYBR Green master mix (Qiagen, Cat. no. 204074, Hilden, Germany), 1 µM of each primer, 10 ng of cDNA, and RNase-free water for a final volume of 10 µL. For PCR amplification, the thermocycler program included a preheating step at 95 °C for 10 min, followed by 40 cycles of denaturation at 95 °C for 30 s, 30 s annealing at 59 °C, and 30 s extension at 72 °C. Dissociation curves were performed at the end of each run to confirm single-product amplifications. Gene-specific primers were designed with Primer3 software (Supplementary Table 1); only primers for the housekeeping gene *CDK* [85] were downloaded from the literature. PCR amplification efficiency of the housekeeping and target genes was determined from standard curves constructed from serial dilutions of cDNA (from 1 to 100 ng). Relative quantification of maize genes was normalized to the housekeeping gene *CDK*, and fold change (FC) values in gene expression were calculated using the comparative threshold cycle method $2^{-\Delta\Delta Ct}$ [86].

 doi:10.20944/preprints202510.2343.v1

4.9. Statistical Analysis

Data on plant growth parameters from the tripartite assay samples were assessed for normality by the Kolmogorov–Smirnov test and then analyzed by one-way ANOVA using the IBM SPSS Statistics v25 software. Differences among treatments were determined by Tukey's test ($P = 0.05$).

5. Conclusion

The transcriptomic analysis of a tripartite interaction model system allowed us to dissect the molecular mechanisms involved in maize roots when interacting with the biocontrol endophytic bacteria B25, the fungal phytopathogen Fv, and both microorganisms simultaneously (Figure 6). In the plant-bacterium interaction (Figure 6a), maize plants appear to recognize B25 as a non-threatening organism, after which the bacterium induces key mechanisms that promote plant growth, preparing the plant for pathogen attack. In the plant-fungus interaction (Figure 6b), the fungal pathogen strongly affected the proper function of plant DNA and protein synthesis machinery, turning off pathways related to these mechanisms. Finally, during the tripartite interaction (Figure 6c), a core of unique genes related to plant defense responses were involved in the successful control of Fv infection, as well as the involvement of genes positively affecting plant growth and development.

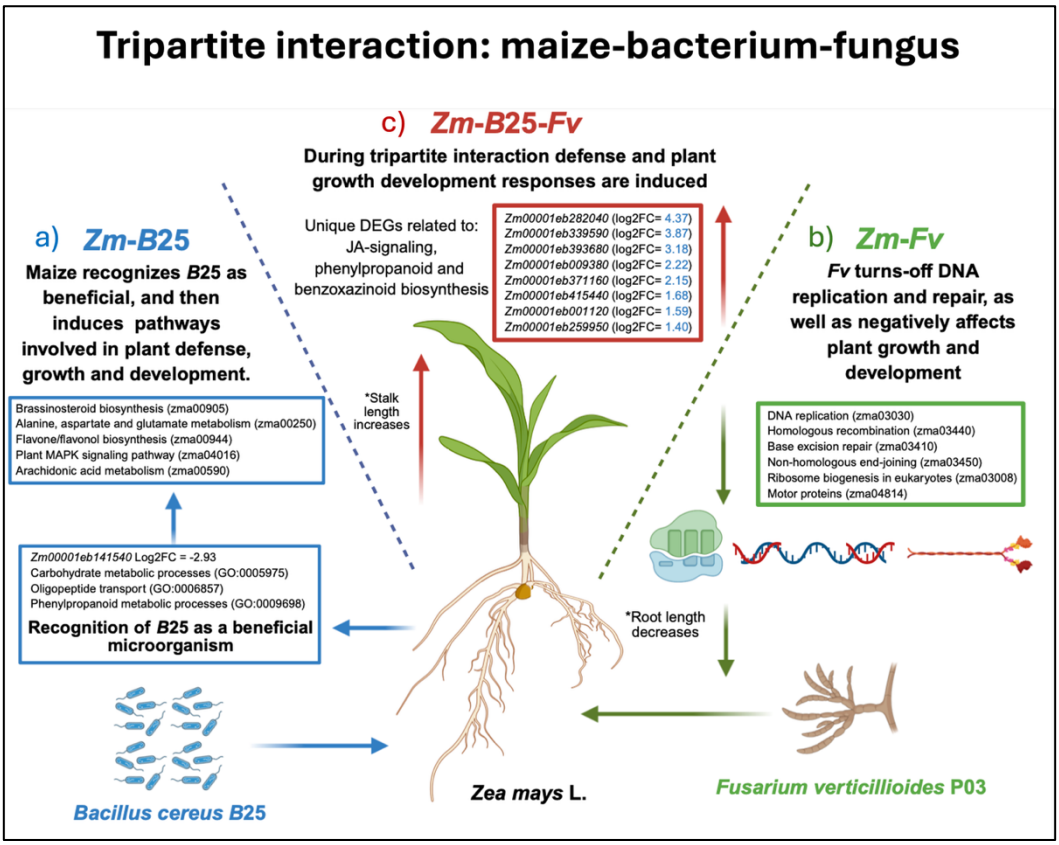

Figure 6. Graphic summary of the main molecular mechanisms involved in maize roots when interacting with the biocontrol endophytic bacterium *B25*, the fungal phytopathogen *Fv*, or both microorganisms (tripartite interaction). a) During the plant-bacterium interaction, *B25* is recognized by maize as a beneficial microorganism and induces the activation of pathways related to plant growth and development as well as defense responses, preparing the plant for pathogen attack. b) During the plant-fungus interaction, *Fv* turns off key mechanisms of plant DNA replication and repair, as well as pathways of ribosome biogenesis and motor proteins; additionally, it negatively affects plant growth and development, decreasing root length. c) During the maize-bacterium-fungus tripartite interaction, several unique DEGs related to defense response and plant growth development are induced. The most induced maize DEGs in the tripartite interaction are shown in the red box.

Supplementary Materials: The following supporting information can be downloaded at the website of this paper posted on Preprints.org. Supplementary Methods. Figure S1: Superficially disinfected maize root pieces showing the growth of *B*25 (red arrows) or *Fv* (green arrows) at 7 dpi, 48 h after incubation on media. Figure S2: Principal component analysis of maize root transcriptional profiles using normalized expression values.; Table S1: Principal component analysis of maize root transcriptional profiles using normalized expression values. Table S2: List of total, common and unique DEGs with log2FoldChange value in and between the interaction conditions from the tripartite experiment. Table S3: Overrepresented GO terms for unique expressed genes from interaction conditions. Table S4: GO Enriched Terms from DEGs of interaction conditions. Table S5: KEGG over-represented Terms of interaction conditions. Table S6: Integration of B73 RefGen_v4 and RefGen_v5 annotations. Table S7: Analysis of non-redundant gene identifiers (NRGIs) using String and Genemania.

Author Contributions: Conceptualization, PABA, ACM and IEMM; methodology, PABA, JECA and ACM; software, ACM and JGJ; validation, PABA, JLFC, IGLS and ACM; formal analysis, PABA, ACM, JLFC, IGLS and JGJ; investigation, PABA, JLFC, IGLS, JECA and ACM; resources, IEMM, ACM and CLCV; data curation, PABA, ACM and IEMM; writing—original draft preparation, PABA, ACM and IEMM; writing—review and editing, JGJ, JLFC, IGLS, CLCV and JECA; visualization, PABA, ACM, IEMM, JLFC and IGLS; supervision, IEMM and ACM.; project administration, IEMM; funding acquisition, IEMM. All authors have read and agreed to the published version of the manuscript.

Funding: This work was supported by SECIHTI FOINS Fronteras de la Ciencia Grant No. 2016-01-2510. PABA was granted a PhD fellowship (No. 70883) from SECIHTI, and JECA received Master's and PhD fellowships (No. 934735) from SECIHTI. PABA and JECA were both granted complementary fellowship support from IPN (BEIFI fellowship program). The OOREAM server at the CIIDIR-IPN Sinaloa was funded by SECIHTI (project 302541).

Data Availability Statement: Raw sequence reads of this study can be downloaded download from https://www.ncbi.nlm.nih.gov/bioproject/PRJNA1345406. The rest of data related to this work are contained within the article.

Acknowledgments: We thank Dr. Brandon Loveall from Improvence editing services for English proofreading of the manuscript.

Conflicts of Interest: The authors declare no conflicts of interest.

References

1. Erenstein, O.; Jaleta, M.; Sonder, K.; Mottaleb, K.; Prasanna, B.M. Global Maize Production, Consumption and Trade: Trends and R&D Implications. *Food Secur* **2022**, doi:10.1007/s12571-022-01288-7.
2. Butrón, A.; Reid, L.M.; Santiago, R.; Cao, A.; Malvar, R.A. Inheritance of Maize Resistance to Gibberella and Fusarium Ear Rots and Kernel Contamination with Deoxynivalenol and Fumonisins. *Plant Pathol* **2015**, *64*, 1053–1060, doi:10.1111/ppa.12351.
3. Subedi, S. A Review on Important Maize Diseases and Their Management in Nepal. *Journal of Maize Research and Development* **2015**, *1*, 28–52, doi:10.3126/jmrd.v1i1.14242.
4. Leyva-Madrigal, K.Y.; Larralde-Corona, C.P.; Apodaca-Sánchez, M.A.; Quiroz-Figueroa, F.R.; Mexia-Bolaños, P.A.; Portillo-Valenzuela, S.; Ordaz-Ochoa, J.; Maldonado-Mendoza, I.E. *Fusarium* Species from the *Fusarium Fujikuroi* Species Complex Involved in Mixed Infections of Maize in Northern Sinaloa, Mexico. *Journal of Phytopathology* **2015**, *163*, 486–497, doi:10.1111/jph.12346.
5. Bacon, C.W.; Glenn, A.E.; Yates, I.E. Fusarium Verticillioides: Managing the Endophytic Association with Maize for Reduced Fumonisins Accumulation. *Toxin Rev* **2008**, *27*, 411–446, doi:10.1080/15569540802497889.
6. Deepa, N.; Nagaraja, H.; Sreenivasa, M.Y. Prevalence of Fumonisin Producing *Fusarium Verticillioides* Associated with Cereals Grown in Karnataka (India). *Food Science and Human Wellness* **2016**, *5*, 156–162, doi:10.1016/j.fshw.2016.07.001.
7. Koul, B.; Chopra, M.; Lamba, S. Microorganisms as Biocontrol Agents for Sustainable Agriculture. *Relationship Between Microbes and the Environment for Sustainable Ecosystem Services, Volume 1* **2022**, 45–68, doi:10.1016/B978-0-323-89938-3.00003-7.

8. De los Santos Villalobos, S.; Parra Cota, F.I.; Herrera Sepúlveda, A.; Valenzuela Aragón, B.; Estrada Mora, J.C. Colmena: Colección de Microorganismos Edáficos y Endófitos Nativos, Para Contribuir a La Seguridad Alimentaria Nacional. *Rev Mex De Cienc Agric* **2018**, *9*, 191–202, doi:10.29312/remexca.v9i1.858.
9. Lizárraga-Sánchez, G.J.; Leyva-Madrigal, K.Y.; Sánchez-Peña, P.; Quiroz-Figueroa, F.R.; Maldonado-Mendoza, I.E. Bacillus Cereus Sensu Lato Strain B25 Controls Maize Stalk and Ear Rot in Sinaloa, Mexico. *Field Crops Res* **2015**, *176*, 11–21, doi:10.1016/j.fcr.2015.02.015.
10. Bacon, C.W.; Hinton, D.M. In Planta Reduction of Maize Seedling Stalk Lesions by the Bacterial Endophyte Bacillus Mojavensis. *Can J Microbiol* **2011**, *57*, 485–492, doi:10.1139/w11-031.
11. Pal, G.; Kumar, K.; Verma, A.; Verma, S.K. Seed Inhabiting Bacterial Endophytes of Maize Promote Seedling Establishment and Provide Protection against Fungal Disease. *Microbiol Res* **2022**, *255*, 126926, doi:10.1016/j.micres.2021.126926.
12. Yang, F.; Zhang, R.; Wu, X.; Xu, T.; Ahmad, S.; Zhang, X.; Zhao, J.; Liu, Y. An Endophytic Strain of the Genus Bacillus Isolated from the Seeds of Maize (Zea Mays L.) Has Antagonistic Activity against Maize Pathogenic Strains. *Microb Pathog* **2020**, *142*, 104074, doi:10.1016/j.micpath.2020.104074.
13. Figueroa-López, A.M.; Cordero-Ramírez, J.D.; Martínez-Álvarez, J.C.; López-Meyer, M.; Lizárraga-Sánchez, G.J.; Félix-Gastélum, R.; Castro-Martínez, C.; Maldonado-Mendoza, I.E. Rhizospheric Bacteria of Maize with Potential for Biocontrol of *Fusarium Verticillioides*. *Springerplus* **2016**, *5*, doi:10.1186/s40064-016-1780-x.
14. Fadiji, A.E.; Babalola, O.O. Elucidating Mechanisms of Endophytes Used in Plant Protection and Other Bioactivities With Multifunctional Prospects. *Front Bioeng Biotechnol* **2020**, *8*, 1–20, doi:10.3389/fbioe.2020.00467.
15. Bolivar-Anillo, H.J.; González-Rodríguez, V.E.; Cantoral, J.M.; García-Sánchez, D.; Collado, I.G.; Garrido, C. Endophytic Bacteria Bacillus Subtilis, Isolated from Zea Mays, as Potential Biocontrol Agent against Botrytis Cinerea. *Biology (Basel)* **2021**, *10*, doi:10.3390/biology10060492.
16. Liu, H.; Carvalhais, L.C.; Crawford, M.; Singh, E.; Dennis, P.G.; Pieterse, C.M.J.; Schenk, P.M. Inner Plant Values: Diversity, Colonization and Benefits from Endophytic Bacteria. *Front Microbiol* **2017**, *8*, 1–17, doi:10.3389/fmicb.2017.02552.
17. Figueroa-López, A.M. Caracterización de Los Mecanismos de Antagonismo Que Emplea Bacillus Cereus Seleccionado Para El Control de Fusarium Verticillioides. Doctoral Thesis, Instituto Politécnico Nacional: Guasave, Sinaloa, 2016.
18. Martínez-Álvarez, J.C.; Castro-Martínez, C.; Sánchez-Peña, P.; Gutiérrez-Dorado, R.; Maldonado-Mendoza, I.E. Development of a Powder Formulation Based on *Bacillus Cereus Sensu Lato* Strain B25 Spores for Biological Control of *Fusarium Verticillioides* in Maize Plants. *World J Microbiol Biotechnol* **2016**, *32*, doi:10.1007/s11274-015-2000-5.
19. Douriet-Gámez, N.R.; Maldonado-Mendoza, I.E.; Ibarra-Laclette, E.; Blom, J.; Calderón-Vázquez, C.L. Genomic Analysis of *Bacillus* Sp. Strain B25, a Biocontrol Agent of Maize Pathogen *Fusarium Verticillioides*. *Curr Microbiol* **2018**, *75*, 247–255, doi:10.1007/s00284-017-1372-1.
20. Morales-Ruiz, E.; Priego-Rivera, R.; Figueroa-López, A.M.; Cazares-Álvarez, J.E.; Maldonado-Mendoza, I.E. Biochemical Characterization of Two Chitinases from Bacillus Cereus Sensu Lato B25 with Antifungal Activity against Fusarium Verticillioides P03. *FEMS Microbiol Lett* **2021**, *368*, 1–8, doi:10.1093/femsle/fnaa218.
21. Báez-Astorga, P.A.; Cázares-Álvarez, J.E.; Cruz-Mendívil, A.; Quiroz-Figueroa, F.R.; Sánchez-Valle, V.I.; Maldonado-Mendoza, I.E. Molecular and Biochemical Characterisation of Antagonistic Mechanisms of the Biocontrol Agent Bacillus Cereus B25 Inhibiting the Growth of the Phytopathogen Fusarium Verticillioides P03 during Their Direct Interaction in Vitro. *Biocontrol Sci Technol* **2022**, 1–21, doi:10.1080/09583157.2022.2085662.
22. Figueroa-López, A.M.; Leyva-Madrigal, K.Y.; Cervantes-Gámez, R.G.; Beltran-Arredondo, L.I.; Douriet-Gámez, N.R.; Castro-Martínez, C.; Maldonado-Mendoza, I.E. Induction of *Bacillus Cereus* Chitinases as a Response to Lysates of *Fusarium Verticillioides*. **2017**, *22*, 12722–12731.

23. Park, Y.S.; Park, J.S.; Lee, S.; Jung, S.H.; Kim, S.K.; Ryu, C.M. Simultaneous Profiling of Arabidopsis Thaliana and Vibrio Vulnificus MO6-24/O Transcriptomes by Dual RNA-Seq Analysis. *Comput Struct Biotechnol J* **2021**, *19*, 2084–2096, doi:10.1016/j.csbj.2021.04.008.
24. Gheler, C.F.; Domingues Zucchi, T.; Soares de Melo, I. Biological Control of Phytopathogenic Fungi by Endophytic Actinomycetes Isolated from Maize (Zea Mays L.). *Brazilian archives of Biology and Technology* **2013**, *56*, 948–955. https://doi.org/10.1590/S1516-89132013000600009
25. Cazares-Álvarez, J.E.; Báez-Astorga, P.A.; Arroyo-Becerra, A.; Maldonado-Mendoza, I.E. Genome-Wide Identification of a Maize Chitinase Gene Family and the Induction of Its Expression by Fusarium Verticillioides (Sacc.) Nirenberg (1976) Infection. *Genes (Basel)* **2024**, *15*, doi:10.3390/genes15081087.
26. Perrot, T.; Pauly, M.; Ramírez, V. Emerging Roles of β-Glucanases in Plant Development and Adaptative Responses. *Plants* **2022**, *11*, doi:10.3390/plants11091119.
27. Zhang, Q.; Zhao, X.; Qiu, H. Flavones and Flavonols: Phytochemistry and Biochemistry. In *Natural Products: Phytochemistry, Botany and Metabolism of Alkaloids, Phenolics and Terpenes*; Ramawat, K.G., Mérillon, J.-M., Eds.; Springer Berlin Heidelberg: Berlin, Heidelberg, 2013; pp. 1821–1847 ISBN 978-3-642-22144-6.
28. Singh, P.; Arif, Y.; Bajguz, A.; Hayat, S. The Role of Quercetin in Plants. *Plant Physiology and Biochemistry* **2021**, *166*, 10–19, doi:10.1016/j.plaphy.2021.05.023.
29. Wang, L.; Chen, M.; Lam, P.Y.; Dini-Andreote, F.; Dai, L.; Wei, Z. Multifaceted Roles of Flavonoids Mediating Plant-Microbe Interactions. *Microbiome* **2022**, *10*, 1–13, doi:10.1186/s40168-022-01420-x.
30. Zhang, H.; Zhao, D.; Tang, Z.; Zhang, Y.; Zhang, K.; Dong, J.; Wang, F. Exogenous Brassinosteroids Promotes Root Growth, Enhances Stress Tolerance, and Increases Yield in Maize. *Plant Signal Behav* **2022**, *17*, 1–14, doi:10.1080/15592324.2022.2095139.
31. Hagen, G.; Guilfoyle, T. Auxin-Responsive Gene Expression: Genes, Promoters and Regulatory Factors. *Plant Mol Biol* **2002**, *49*, 373–385, doi:10.1023/A:1015207114117.
32. Franco, A.R.; Gee, M.A.; Guilfoyle, T.J. Induction and Superinduction of Auxin-Responsive MRNAs with Auxin and Protein Synthesis Inhibitors. *J Biol Chem* **1990**, *265*, 15845–15849, doi.org/10.1016/S0021-9258(18)55475-2
33. Sowmya, R.S.; Warke, V.G.; Mahajan, G.B.; Annapure, U.S. Effect of Amino Acids on Growth, Elemental Content, Functional Groups, and Essential Oils Composition on Hydroponically Cultivated Coriander under Different Conditions. *Ind Crops Prod* **2023**, *197*, 116577, doi:10.1016/j.indcrop.2023.116577.
34. Colla, G.; Nardi, S.; Cardarelli, M.; Ertani, A.; Lucini, L.; Canaguier, R.; Rouphael, Y. Protein Hydrolysates as Biostimulants in Horticulture. *Sci Hortic* **2015**, *196*, 28–38, doi:10.1016/j.scienta.2015.08.037.
35. Alfosea-Simón, M.; Simón-Grao, S.; Zavala-Gonzalez, E.A.; Cámara-Zapata, J.M.; Simón, I.; Martínez-Nicolás, J.J.; Lidón, V.; García-Sánchez, F. Physiological, Nutritional and Metabolomic Responses of Tomato Plants After the Foliar Application of Amino Acids Aspartic Acid, Glutamic Acid and Alanine. *Front Plant Sci* **2021**, *11*, 1–16, doi:10.3389/fpls.2020.581234.
36. Islam, M.M.; Hassan, M.U.; Ishfaq, M.; Ripa, F.A.; Nadeem, F.; Ahmad, Z.; Xu, J.; Ning, P.; Li, X. Foliar Glutamine Application Improves Grain Yield and Nutritional Quality of Field-Grown Maize (Zea Mays L.) Hybrid ZD958. *J Plant Growth Regul* **2024**, *43*, 624–637, doi:10.1007/s00344-023-11121-w.
37. Xu, J.; Zhang, S. Mitogen-Activated Protein Kinase Cascades in Signaling Plant Growth and Development. *Trends Plant Sci* **2015**, *20*, 56–64, doi:10.1016/j.tplants.2014.10.001.
38. Lin, L.; Wu, J.; Jiang, M.; Wang, Y. Plant Mitogen-activated Protein Kinase Cascades in Environmental Stresses. *Int J Mol Sci* 2021, *22*, 1–24, doi.org/10.3390/ijms22041543
39. Dedyukhina, E.G.; Kamzolova, S. V.; Vainshtein, M.B. Arachidonic Acid as an Elicitor of the Plant Defense Response to Phytopathogens. *Chemical and Biological Technologies in Agriculture* **2014**, *1*, 2–7, doi:10.1186/s40538-014-0018-9.
40. Savchenko, T.; Walley, J.W.; Chehab, E.W.; Xiao, Y.; Kaspi, R.; Pye, M.F.; Mohamed, M.E.; Lazarus, C.M.; Bostock, R.M.; Dehesh, K. Arachidonic Acid: An Evolutionarily Conserved Signaling Molecule Modulates Plant Stress Signaling Networks. *Plant Cell* **2010**, *22*, 3193–3205, doi:10.1105/tpc.110.073858.
41. Dye, S.M.; Bostock, R.M. Eicosapolyenoic Fatty Acids Induce Defense Responses and Resistance to Phytophthora Capsici in Tomato and Pepper. *Physiol Mol Plant Pathol* **2021**, *114*, 101642, doi:10.1016/j.pmpp.2021.101642.

42. Lewis, D.C.; van der Zwan, T.; Richards, A.; Little, H.; Coaker, G.L.; Bostock, R.M. The Oomycete Microbe-Associated Molecular Pattern, Arachidonic Acid, and an Ascophyllum Nodosum-Derived Plant Biostimulant Induce Defense Metabolome Remodeling in Tomato. *Phytopathology* **2023**, *113*, 1084–1092, doi:10.1094/PHYTO-10-22-0368-R.
43. Hyong, W.C.; Byung, G.L.; Nak, H.K.; Park, Y.; Chae, W.L.; Hyun, K.S.; Byung, K.H. A Role for a Menthone Reductase in Resistance against Microbial Pathogens in Plants. *Plant Physiol* **2008**, *148*, 383–401, doi:10.1104/pp.108.119461.
44. Dias, M.C.; Pinto, D.C.G.A.; Silva, A.M.S. Plant Flavonoids: Chemical Characteristics and Biological Activity. *Molecules* 2021, *26*, doi.org/10.3390/molecules26175377
45. Wang, Y.; Zhou, L.J.; Wang, Y.; Liu, S.; Geng, Z.; Song, A.; Jiang, J.; Chen, S.; Chen, F. Functional Identification of a Flavone Synthase and a Flavonol Synthase Genes Affecting Flower Color Formation in Chrysanthemum Morifolium. *Plant Physiology and Biochemistry* **2021**, *166*, 1109–1120, doi:10.1016/j.plaphy.2021.07.019.
46. Alseekh, S.; Perez de Souza, L.; Benina, M.; Fernie, A.R. The Style and Substance of Plant Flavonoid Decoration; towards Defining Both Structure and Function. *Phytochemistry* 2020, *174*, doi.org/10.1016/j.phytochem.2020.112347
47. Manova, V.; Gruszka, D. DNA Damage and Repair in Plants – From Models to Crops. *Front Plant Sci* **2015**, *6*, 1–26, doi:10.3389/fpls.2015.00885.
48. Nisa, M.U.; Huang, Y.; Benhamed, M.; Raynaud, C. The Plant DNA Damage Response: Signaling Pathways Leading to Growth Inhibition and Putative Role in Response to Stress Conditions. *Front Plant Sci* **2019**, *10*, 1–12, doi:10.3389/fpls.2019.00653.
49. Grin, I.R.; Petrova, D. V.; Endutkin, A. V.; Ma, C.; Yu, B.; Li, H.; Zharkov, D.O. Base Excision DNA Repair in Plants: Arabidopsis and Beyond. *Int J Mol Sci* **2023**, *24*, doi:10.3390/ijms241914746.
50. Szurman-Zubrzycka, M.; Jędrzejek, P.; Szarejko, I. How Do Plants Cope with DNA Damage? A Concise Review on the DDR Pathway in Plants. *Int J Mol Sci* **2023**, *24*, doi:10.3390/ijms24032404.
51. Guo, Z.; Wang, X.; Li, Y.; Xing, A.; Wu, C.; Li, D.; Wang, C.; de Bures, A.; Zhang, Y.; Guo, S.; et al. Arabidopsis SMO2 Modulates Ribosome Biogenesis by Maintaining the RID2 Abundance during Organ Growth. *Plant Journal* **2023**, *114*, 96–109, doi:10.1111/tpj.16121.
52. Nebenführ, A.; Dixit, R. Kinesins and Myosins: Molecular Motors That Coordinate Cellular Functions in Plants. *Annu Rev Plant Biol* **2018**, *69*, 329–361, doi:10.1146/annurev-arplant-042817-040024.
53. Li, J.; Xu, Y.; Chong, K. The Novel Functions of Kinesin Motor Proteins in Plants. *Protoplasma* 2012, *249*, 95–100, doi.org/10.1007/s00709-011-0357-3
54. Ryan, J.M.; Nebenführ, A. Update on Myosin Motors: Molecular Mechanisms and Physiological Functions. *Plant Physiol* 2018, *176*, 119–127, doi.org/10.1104/pp.17.01429
55. Mao, L.; Ge, L.; Ye, X.; Xu, L.; Si, W.; Ding, T. ZmGLP1, a Germin-like Protein from Maize, Plays an Important Role in the Regulation of Pathogen Resistance. *Int J Mol Sci* **2022**, *23*, doi:10.3390/ijms232214316.
56. Khare, D.; Choi, H.; Huh, S.U.; Bassin, B.; Kim, J.; Martinoia, E.; Sohn, K.H.; Paek, K.H.; Lee, Y.; Chrispeels, M.J. Arabidopsis ABCG34 Contributes to Defense against Necrotrophic Pathogens by Mediating the Secretion of Camalexin. *Proc Natl Acad Sci U S A* **2017**, *114*, E5712–E5720, doi:10.1073/pnas.1702259114.
57. Li, M.R.; Qi, X.; Li, D.; Wu, Z.; Liu, M.; Yang, W.; Zang, Z.; Jiang, L. Comparative Transcriptome Analysis Highlights Resistance Regulatory Networks of Maize in Response to Exserohilum Turcicum Infection at the Early Stage. *Physiol Plant* **2024**, *176*, doi:10.1111/ppl.14615.
58. Shumayla; Madhu; Singh, K.; Upadhyay, S.K. LysM Domain-Containing Proteins Modulate Stress Response and Signalling in Triticum Aestivum L. *Environ Exp Bot* **2021**, *189*, doi:10.1016/j.envexpbot.2021.104558.
59. Giovannoni, M.; Lironi, D.; Marti, L.; Paparella, C.; Vecchi, V.; Gust, A.A.; De Lorenzo, G.; Nürnberger, T.; Ferrari, S. The Arabidopsis Thaliana LysM-Containing Receptor-Like Kinase 2 Is Required for Elicitor-Induced Resistance to Pathogens. *Plant Cell Environ* **2021**, *44*, 3545–3562, doi:10.1111/pce.14192.
60. Kumar, R.; Meghwanshi, G.K.; Marcianò, D.; Ullah, S.F.; Bulone, V.; Toffolatti, S.L.; Srivastava, V. Sequence, Structure and Functionality of Pectin Methylesterases and Their Use in Sustainable Carbohydrate Bioproducts: A Review. *Int J Biol Macromol* **2023**, *244*, doi:10.1016/j.ijbiomac.2023.125385.

61. Zhou, S.; Richter, A.; Jander, G. Beyond Defense: Multiple Functions of Benzoxazinoids in Maize Metabolism. *Plant Cell Physiol* 2018, *59*, 1528–1533, 10.1093/pcp/pcy064
62. Lee, J.R.; Boltz, K.A.; Lee, S.Y. Molecular Chaperone Function of Arabidopsis Thaliana Phloem Protein 2-A1, Encodes a Protein Similar to Phloem Lectin. *Biochem Biophys Res Commun* **2014**, *443*, 18–21, doi:10.1016/j.bbrc.2013.11.034.
63. Zheng, L.; Zheng, H.; Zheng, X.; Duan, Y.; Yu, X. PP2 Gene Family in Phyllostachys Edulis: Identification, Characterization, and Expression Profiles. *BMC Genomics* **2024**, *25*, doi:10.1186/s12864-024-11007-5.
64. Bao, Y.; Song, W.M.; Pan, J.; Jiang, C.M.; Srivastava, R.; Li, B.; Zhu, L.Y.; Su, H.Y.; Gao, X.S.; Liu, H.; et al. Overexpression of the NDR1/HIN1-Like Gene NHL6 Modifies Seed Germination in Response to Abscisic Acid and Abiotic Stresses in Arabidopsis. *PLoS One* **2016**, *11*, doi:10.1371/journal.pone.0148572.
65. Maldonado, A.; Youssef, R.; McDonald, M.; Brewer, E.; Beard, H.; Matthews, B. Overexpression of Four Arabidopsis Thaliana NHL Genes in Soybean (Glycine Max) Roots and Their Effect on Resistance to the Soybean Cyst Nematode (Heterodera Glycines). *Physiol Mol Plant Pathol* **2014**, *86*, 1–10, doi:10.1016/J.PMPP.2014.02.001.
66. Block, A.K.; Tang, H. V.; Hopkins, D.; Mendoza, J.; Solemslie, R.K.; du Toit, L.J.; Christensen, S.A. A Maize Leucine-Rich Repeat Receptor-like Protein Kinase Mediates Responses to Fungal Attack. *Planta* **2021**, *254*, doi:10.1007/s00425-021-03730-0.
67. Ding, N.; Zhao, Y.; Wang, W.; Liu, X.; Shi, W.; Zhang, D.; Chen, J.; Ma, S.; Sun, Q.; Wang, T.; et al. Transcriptome Analysis in Contrasting Maize Inbred Lines and Functional Analysis of Five Maize NAC Genes under Drought Stress Treatment. *Front Plant Sci* **2023**, *13*, doi:10.3389/fpls.2022.1097719.
68. Sun, Y.; Shi, M.; Wang, D.; Gong, Y.; Sha, Q.; Lv, P.; Yang, J.; Chu, P.; Guo, S. Research Progress on the Roles of Actin-Depolymerizing Factor in Plant Stress Responses. *Front Plant Sci* 2023, *14*, doi.org/10.3389/fpls.2023.1278311
69. Shigeyama, T.; Watanabe, A.; Tokuchi, K.; Toh, S.; Sakurai, N.; Shibuya, N.; Kawakami, N. α-Xylosidase Plays Essential Roles in Xyloglucan Remodelling, Maintenance of Cell Wall Integrity, and Seed Germination in Arabidopsis Thaliana. *J Exp Bot* **2016**, *67*, 5615–5629, doi:10.1093/jxb/erw321.
70. White-Gilbertson, S.; Rubinchik, S.; Voelkel-Johnson, C. Transformation, Translation and TRAIL: An Unexpected Intersection. *Cytokine Growth Factor Rev* **2008**, *19*, 167–172, doi:10.1016/j.cytogfr.2008.01.007.
71. Xie, Y.; Wang, Y.; Yu, X.; Lin, Y.; Zhu, Y.; Chen, J.; Xie, H.; Zhang, Q.; Wang, L.; Wei, Y.; et al. SH3P2, an SH3 Domain-Containing Protein That Interacts with Both Pib and AvrPib, Suppresses Effector-Triggered, Pib-Mediated Immunity in Rice. *Mol Plant* **2022**, *15*, 1931–1946, doi:10.1016/J.MOLP.2022.10.022.
72. Jasim, B.; Joseph, A.A.; John, C.J.; Mathew, J.; Radhakrishnan, E.K. Isolation and Characterization of Plant Growth Promoting Endophytic Bacteria from the Rhizome of Zingiber Officinale. *3 Biotech* **2014**, *4*, 197–204, doi:10.1007/s13205-013-0143-3.
73. Aranda, P.S.; Lajoie, D.M.; Jorcyk, C.L. Bleach Gel: A Simple Agarose Gel for Analyzing RNA Quality. *Electrophoresis* **2012**, *33*, 366–369, doi:10.1002/elps.201100335.
74. Bolger, A.M.; Lohse, M.; Usadel, B. Trimmomatic: A Flexible Trimmer for Illumina Sequence Data. *Bioinformatics* **2014**, *30*, 2114–2120, doi:10.1093/bioinformatics/btu170.
75. Woodhouse, M.R.; Cannon, E.K.; Portwood, J.L.; Harper, L.C.; Gardiner, J.M.; Schaeffer, M.L.; Andorf, C.M. A Pan-Genomic Approach to Genome Databases Using Maize as a Model System. *BMC Plant Biol* **2021**, *21*, doi:10.1186/s12870-021-03173-5.
76. Dobin, A.; Davis, C.A.; Schlesinger, F.; Drenkow, J.; Zaleski, C.; Jha, S.; Batut, P.; Chaisson, M.; Gingeras, T.R. STAR: Ultrafast Universal RNA-Seq Aligner. *Bioinformatics* **2013**, *29*, 15–21, doi:10.1093/bioinformatics/bts635.
77. Anders, S.; Pyl, P.T.; Huber, W. HTSeq-A Python Framework to Work with High-Throughput Sequencing Data. *Bioinformatics* **2015**, *31*, 166–169, doi:10.1093/bioinformatics/btu638.
78. Love, M.I.; Huber, W.; Anders, S. Moderated Estimation of Fold Change and Dispersion for RNA-Seq Data with DESeq2. *Genome Biol* **2014**, *15*, 1–21, doi:10.1186/s13059-014-0550-8.
79. Martin, F.J.; Amode, M.R.; Aneja, A.; Austine-Orimoloye, O.; Azov, A.G.; Barnes, I.; Becker, A.; Bennett, R.; Berry, A.; Bhai, J.; et al. Ensembl 2023. *Nucleic Acids Res* **2023**, *51*, D933–D941, doi:10.1093/nar/gkac958.

 doi:10.20944/preprints202510.2343.v1

80. Young, M.D.; Wakefield, M.J.; Smyth, G.K.; Oshlack, A. Gene Ontology Analysis for RNA-Seq: Accounting for Selection Bias. *Genome Biol* **2010**, *11*, doi:10.1186/gb-2010-11-2-r14.
81. Tian, T.; Liu, Y.; Yan, H.; You, Q.; Yi, X.; Du, Z.; Xu, W.; Su, Z. AgriGO v2.0: A GO Analysis Toolkit for the Agricultural Community, 2017 Update. *Nucleic Acids Res* **2017**, *45*, W122–W129, doi:10.1093/nar/gkx382.
82. Szklarczyk, D.; Gable, A.L.; Lyon, D.; Junge, A.; Wyder, S.; Huerta-Cepas, J.; Simonovic, M.; Doncheva, N.T.; Morris, J.H.; Bork, P.; et al. STRING V11: Protein–Protein Association Networks with Increased Coverage, Supporting Functional Discovery in Genome-Wide Experimental Datasets. *Nucleic Acids Res* **2019**, *47*, D607–D613, doi:10.1093/nar/gky1131.
83. Warde-Farley, D.; Donaldson, S.L.; Comes, O.; Zuberi, K.; Badrawi, R.; Chao, P.; Franz, M.; Grouios, C.; Kazi, F.; Lopes, C.T.; et al. The GeneMANIA Prediction Server: Biological Network Integration for Gene Prioritization and Predicting Gene Function. *Nucleic Acids Res* **2010**, *38*, W214–W220, doi:10.1093/nar/gkq537.
84. Shannon, P.; Markiel, A.; Ozier, O.; Baliga, N.S.; Wang, J.T.; Ramage, D.; Amin, N.; Schwikowski, B.; Ideker, T. Cytoscape: A Software Environment for Integrated Models of Biomolecular Interaction Networks. *Genome Res* **2003**, *13*, 2498–2504, doi:10.1101/gr.1239303.
85. Lin, F.; Jiang, L.; Liu, Y.; Lv, Y.; Dai, H.; Zhao, H. Genome-Wide Identification of Housekeeping Genes in Maize. *Plant Mol Biol* **2014**, *86*, 543–554, doi:10.1007/s11103-014-0246-1.
86. Livak, K.J.; Schmittgen, T.D. Analysis of Relative Gene Expression Data Using Real-Time Quantitative PCR and the 2−ΔΔCT Method. *Methods* **2001**, *25*, 402–408, doi:https://doi.org/10.1006/meth.2001.1262.